(+)-catechin attenuates multiple atherosclerosis-associated processes *in vitro,* modulates disease-associated risk factors in C57BL/6J mice and reduces atherogenesis in LDL receptor deficient mice by inhibiting inflammation and increasing markers of plaque stability

Yee-Hung Chan[1], Joe W. E. Moss[1], Jessica O. Williams[1], Nele Ferekidis[1], Nouf Alshehri[1], Timothy R. Hughes[2], Juan B. Menendez-Gonzalez[3], Sue F. Plummer[4], Daryn R. Michael[4] Neil P. Rodrigues[3], and Dipak P. Ramji[1*].

[1]Cardiff School of Biosciences, Cardiff University, Sir Martin Evans Building, Museum Avenue, Cardiff CF10 3AX, UK.

[2]Division of Infection and Immunity, Henry Wellcome Building, School of Medicine, Cardiff University, Heath Park, Cardiff CF14 4XN, UK.

[3]European Cancer Stem Cell Research Institute, Cardiff School of Biosciences, Cardiff University, Hadyn Ellis Building, Maindy Road, Cardiff CF24 4HQ, UK.

[4]Cultech Limited, Unit 2 Christchurch Road, Baglan Industrial Park, Port Talbot SA12 7BZ, UK.

Key words: Atherosclerosis; (+)-catechin; gene expression; macrophages; nutraceuticals; plaque stability

Received: MONTH DD, YYY; Revised: MONTH DD, YYY; Accepted: MONTH DD, YYY

This article has been accepted for publication and undergone full peer review but has not been through the copyediting, typesetting, pagination and proofreading process, which may lead to differences between this version and the Version of Record. Please cite this article as doi: 10.1002/mnfr.202200716.

***Corresponding author:** Professor Dipak P. Ramji, Cardiff School of Biosciences, Cardiff University, Sir Martin Evans Building, Museum Avenue, Cardiff CF10 3AX, UK. Tel: 0044 (0)29 20876753; Fax: Email: Ramji@Cardiff.ac.uk

Abstract

Scope: A prospective study of 34,492 participants showed an inverse association between (+)-catechin intake and coronary heart disease. The effects of (+)-catechin on atherosclerosis and associated risk factors are poorly understood and were investigated.

Methods and Results: (+)-catechin attenuates reactive oxygen species production in human macrophages, endothelial cells and vascular smooth muscle cells, chemokine-driven monocytic migration, and proliferation of human macrophages and their expression of several pro-atherogenic genes. (+)-catechin also improves oxidized LDL-mediated mitochondrial membrane depolarization in endothelial cells and attenuates growth factor-induced smooth muscle cell migration. In C57BL/6J mice fed high fat diet (HFD) for 3 weeks, (+)-catechin attenuates plasma levels of triacylglycerol and interleukin (IL)-1β and IL-2, produces anti-atherogenic changes in liver gene expression, and reduces levels of white blood cells, myeloid-derived suppressor cells, Lin^- Sca^+ c-Kit^+ cells and common lymphoid progenitor cells within the bone marrow. In LDL receptor deficient mice fed HFD for 12 weeks, (+)-catechin attenuates atherosclerotic plaque burden and inflammation with reduced macrophage content and increased markers of plaque stability, smooth muscle cells and collagen.

Conclusion: This study provides novel, detailed insights into the cardio-protective actions of (+)-catechin together with underlying molecular mechanisms and supports further assessments of its beneficial effects in human trials.

1. Introduction

Atherosclerosis, an inflammatory disorder of the vasculature, is the underlying cause of cardiovascular disease (CVD) [1]. Atherosclerosis is initiated by endothelial cell dysfunction/activation in response to risk factors such as hypercholesterolemia, which leads to the accumulation of low-density lipoproteins (LDL) within the arterial wall, hypertension, smoking, obesity, diabetes and diet rich in saturated fats [1]. This results in a series of events [1-6] that include: (i) recruitment of immune cells, particularly monocytes, into the subendothelial space in response to chemokines from endothelial cells and expression of adhesion proteins on their cell surface; (ii) differentiation of monocytes into macrophages and their subsequent transformation into foam cells via the uptake of LDL and modified LDL; (iii) lysis of foam cells leading to formation of lipid-rich necrotic core; (iv) chronic inflammation orchestrated by cytokines; (v) proliferation and migration of smooth muscle cells from the media to the intima to form plaque stabilizing fibrous cap containing extracellular matrix (ECM) secreted by these cells; and (vi) rupture of plaques in response to matrix metalloproteinases (MMP) and other proteases during inflammatory conditions followed by thrombosis and clinical complications such as myocardial infarction and cerebrovascular accident.

Current therapies against atherosclerosis are not fully effective and associated with considerable residual CVD risk and adverse side effects in some patients [1, 2]. For alternative pharmaceutical therapies, some success has been achieved with agents that target dyslipidaemia and inflammation [1, 2]. However, many pharmaceutical leads against established targets (e.g., inhibitors of cholesterol ester transfer protein) have failed in clinical trials [2]. Nutraceuticals have excellent safety profiles but thorough understanding of molecular mechanisms underlying their beneficial actions is often lacking [1, 2].

Diets rich in fruits and vegetables are linked with cardiovascular benefits [1, 7, 8]. However, micro-/macro-nutrients in these foods that are responsible for the protective effects

have been poorly investigated. Catechins are a class of flavonoids present at high levels in plant-based foods [1]. They reduce blood pressure, improve flow-mediated vasodilation and inhibit platelet aggregation [9]. A prospective study of 34,492 participants showed a strong inverse association between the intake of (+)-catechin and (-)-epicatechin and coronary heart disease [10]. The Cocoa Supplement and Multivitamin Outcomes Study (COSMOS) of 21,000 participants also showed that supplementation with cocoa extracts rich in catechins reduced CVD death by 27% in older adults [11]. In addition, studies in apolipoprotein E deficient (*ApoE*$^{-/-}$) or *ApoE**3-Leiden mouse models of atherosclerosis revealed protective actions of catechins, in particular (-)-epicatechin, epigallocatechin-3-gallate (EGCG) and tea catechins [12-16]. Although these and other studies demonstrate anti-atherogenic actions of some catechins *in vitro* and *in vivo*, they provide limited mechanistic insights. Furthermore, individual nutraceutical agents belonging to the same group/class may possess differential beneficial effects and thus underlying mechanisms, depending on variations in their molecular structure affecting absorption and metabolism. In addition, to our knowledge, only two studies have been performed on (+)-catechin alone in a mouse model of atherosclerosis *in vivo* [17, 18]. Furthermore, there have been no studies in the LDL receptor deficient (*LDLr*$^{-/-}$) mouse model that develops mild atherosclerosis following long-term feeding of a chow diet, which can be speeded up to development of more advanced plaques following dietary modification in the form of HFD feeding. This model is hence less aggressive and more akin to diet-induced atherosclerosis in humans, including plasma lipoprotein profile, compared to the *ApoE*$^{-/-}$ model. For example, *ApoE*$^{-/-}$ mice, but not *Ldlr*$^{-/-}$ mice can develop atherosclerosis following long-term feeding of standard chow diet, the disease occurs more rapidly on HFD in *ApoE*$^{-/-}$ mice compared to *Ldlr*$^{-/-}$ mice and the former is associated with increases in plasma very low-density lipoprotein (VLDL) and chylomicron fractions compared to LDL in the latter [19]. In addition, ApoE is involved in the control of several key processes, such as inflammation (i.e., is anti-inflammatory), which may therefore impact plaque development in *ApoE*$^{-/-}$ mice [19]. It is therefore important that further studies are carried out on the anti-atherogenic potential of (+)-catechin and the molecular mechanisms underlying its actions in

different model systems in light of its positive effects in a prospective study of 34,492 patients and the COSMOS trial (21,000 participants) detailed above. We have hence investigated the effect of (+)-catechin on key atherosclerosis-associated processes using cell culture model systems, together with key markers of the disease and gene expression profile in C57BL/6J mice fed HFD and atherosclerosis development and progression in the *LDLr*$^{-/-}$ model system.

2. Materials and Methods

2.1. Reagents

Human monocytic THP-1 cell line, human umbilical cord endothelial cells (HUVEC), human aortic smooth muscle cells (HASMC), (+)-catechin (≥99.0%) and (+)-catechin hydrate (≥98.0%) were from Sigma-Aldrich. Lactate dehydrogenase (LDH) assay kit was from ThermoFisher Scientific; Lymphoprep™ - from Stemcell Technologies; monocyte chemotactic protein-1 (MCP-1), interferon-γ (IFN-γ), tumour necrosis factor-α (TNF-α) and macrophage-colony stimulating factor (M-CSF) - from Peprotech; and oxidized LDL (oxLDL) - from Alfa Aesar. All other reagents were from Sigma-Aldrich unless otherwise stated.

2.2. Cell Culture

Human monocyte-derived macrophages (HMDM) were obtained from monocytes of buffy coats (Welsh Blood Service) using Ficoll-Hypaque purification followed by differentiation in the presence of 20 ng/ml M-CSF for 4-6 days as previously described [20]. Ethical approval and informed consent for each donor was granted to the Welsh Blood Service for use of human blood samples for research. THP-1 cells and HMDM were cultured in RPMI-1640 medium with L-glutamine, 10% (v/v) heat-inactivated foetal calf serum (HI-FCS), penicillin (100 U/ml) and streptomycin (100 µg/ml) at 37ºC in a humidified incubator containing 5% (v/v) CO_2 [20]. Differentiation of THP-1 cells into macrophages was performed

by incubation for 24 h with 0.16 μM of phorbol 12-myristate 13-acetate [16]. HASMC and HUVEC were cultured in their respective ready-to-use media as described by the manufacturers (Sigma-Aldrich) [20].

2.3. *In vitro assays*

Cell proliferation was assessed using crystal violet as in our previous studies [20, 21], counting numbers of cells or using the 5'-bromo-2'-deoxy-uridine labelling and detection kit III, as described by the manufacturers (Sigma-Aldrich). For apoptosis, cells were incubated with vehicle or (+)-catechin for 3 h in serum-free medium containing TNF-α (100 ng/ml). Apoptosis was then determined using the Annexin-V-FITC apoptosis detection kit, as described by the manufacturers (Abcam).

The production of ROS *in vitro* was determined using fluorescent-based 2'7'-dichlorofluorescin diacetate (DCFDA) Cellular ROS Detection Assay Kit (ab113851) using a microplate reader according to the manufacturer's instructions (Abcam). Tert-butyl hydroperoxide (TBHP) was used to stimulate ROS production in cells [20, 22]. Total MMP activity in cell supernatants was determined using fluorescence resonance energy transfer-based assay according to the manufacturer's instructions (Abcam). The uptake of 1,1′-dioctadecyl-3,3,3′,3′-tetramethyllindocarbocyane perchlorate (DiI)-labelled oxLDL and efflux of radiolabelled cholesterol from foam cells was determined as in our previous studies [20, 21]. Changes in mitochondrial membrane potential were monitored using tetraethylbenzimidazolylcarbocyanine iodide (JC-1) that accumulates in energized mitochondria, as described by the manufacturer (Abcam). MCP-1-mediated migration of monocytes and platelet-derived growth factor-mediated migration of HASMC was performed using the modified Boyden chamber, as given in our previous studies [20, 21].

2.4. Gene expression analysis

Atherosclerosis RT^2 Profiler PCR Arrays (Qiagen) were performed as in our previous studies [20-22]. The transcript levels were determined using comparative Ct method and

normalized to housekeeping genes that showed the most stable expression. Real-time quantitative PCR (RT-qPCR) was performed as described in our previous studies [20, 21] using primers shown in Supplementary Table 1.

2.5. Animal experiments

All studies and protocols were approved by Cardiff University Institutional Ethics Review Committee and United Kingdom Home Office and performed in accordance with Guide for Care and Use of Laboratory Animals (NIH Publication No. 85–23, revised 1996; Experimental licence 30/3365). Male C57BL/6J and *LDLr*$^{-/-}$ (homozygous for the *LDLrtm1Her* mutation and backcrossed to the C57BL/6J strain) mice were expanded locally in pathogen-free environment and 8-week-old mice housed in light and temperature-controlled facility (lights on 7 am to 7 pm, 22°C) were used. *LDLr*$^{-/-}$ mice were randomly assigned into two groups and received HFD [21% (w/w) pork lard and 0.15% (w/w) cholesterol] supplemented with either vehicle (PBS) or 200 mg/kg/day (+)-catechin hydrate for 12 weeks (20-25 animals per group) [20]. C57BL/6J mice were randomly assigned to two groups and fed HFD for 3 weeks with daily gavage of either vehicle or 200 mg/kg/day (+)-catechin hydrate (8 animals per group), as in our previous studies [22, 23]. Mice were sacrificed via exposure to increasing CO_2 levels in a chamber and death confirmed by exsanguination (via cardiac puncture). Fat pads and various organs were weighted, snap frozen and stored at -80^{0}C. For *LDLr*$^{-/-}$ mice, hearts were gently perfused with PBS and mounted with Optimum Cutting Temperature (OCT; ThermoFisher) embedding matrix and flash frozen for cryosectioning.

Blood was collected in tubes containing 50 U/ml heparin, and plasma was obtained via centrifugation (12,000 *x g* for 10 min). Plasma levels of total cholesterol, LDL/VLDL and high-density lipoproteins (HDL) were determined using the Cholesterol Assay Kit -HDL (ab65390) (esterase enzyme added to the reaction), whereas triacylglycerol (TG) levels were measured using Triglyceride Assay Kit (ab65336) according to manufacturer's instructions (Abcam) [20, 24]. Cytokine levels were determined by Central Biotechnology

Services (School of Medicine, Cardiff University, UK) using a V-PLEX Plus Pro-inflammatory Panel1 Mouse Kit (Meso Scale Discovery) [21, 22].

2.6. Analysis of hematopoietic stem and progenitor cell populations within the bone marrow (BM)

Immunophenotyping of BM cell populations was performed as carried out in our previous studies [20, 22]. Thus, 10 million, 8 million and 1 million cells were used to analyse signaling lymphocytic activation molecule (SLAM), progenitor cell populations and cell lineage populations, respectively, on a BD LSR Fortessa 4 laser flow cytometer with data analysis carried out using FlowJo software (see Supplementary Table 2 for sources of all antibodies used) [20, 22].

2.7. Atherosclerotic lesion analysis

Sequential 8 µm-thick sections of aortic root were cut at -15°C using a microtome-cryostat starting from three valve cusps, collected onto poly-L-lysine coated slides (VWR, Lutterworth, UK) and air-dried for 1 h prior to storage at -80ºC [20, 25]. Plaque size and lipid content were assessed following Oil red O (ORO) staining whilst Van Gieson's stain was used to determine plaque collagen content as in our previous studies [20, 25, 26]. Plaque cellular composition/immune cell infiltration was assessed via immunofluorescent staining, as performed in our previous studies (see Supplementary Table 3 for antibodies) [20, 21, 26]. All image analyses were performed in a blinded manner using ImageJ software [25, 26]. Plaque size, occlusion and lipid content were calculated using ORO-stained sections [20, 21, 25, 26]; plaque necrosis was quantified using same sections as described by [27]; and plaque stability index was calculated using the following formula: (sum of smooth muscle cell and collagen areas)/(sum of macrophage and lipid areas) as described in [28].

2.8 Statistical analysis

Shapiro-Wilk test, histograms and Q-Q plots were used for evaluating normality of data and any data transformations have been stated. Outliers (data values beyond two standard deviations of the mean) were removed before statistical analysis. Unpaired Student's t test (normal distribution) with (unequal variances) or without (equal variances) Welch's correction, or a Mann-Whitney U test (abnormal distribution) were used for comparisons between two groups. For multiple groups, one-way analysis of variance (ANOVA) was used with appropriate post-hoc tests (Tukey's or Dunnett if variances between different test groups were equal, or Dunnett T3 or Games-Howell in cases of unequal variances). A generalised linear model (GLM) was employed in the cases where a combination of continuous and categorical variables was assessed simultaneously, [22]. Where necessary a generalised linear mixed model (GLMM) was used to avoid pseudo-replication. Significance was defined as $p \leq 0.05$.

3.0. Results

3.1. (+)-catechin attenuates ROS production in human macrophages, endothelial cells and vascular smooth muscle cells

Oxidation of LDL by ROS is a critical event in atherogenesis [2, 4]. The effect of several concentrations of (+)-catechin (based on published literature) on ROS production induced by TBHP (i.e., mimicking ROS production in pathological conditions) in human THP-1 monocytes and macrophages was therefore determined. The THP-1 cell line is used extensively for study of human monocytes and macrophages with demonstrated conservation of responses with primary cultures and *in vivo* [20]. The TBHP-induced ROS production was significantly attenuated by all concentrations of (+)-catechin in both human monocytes and macrophages ($p \leq 0.001$ and $p = 0.021$ respectively for 1.5 μg/ml; $p \leq 0.001$ and $p = 0.001$ respectively for 5 μg/ml; $p \leq 0.001$ in both cases for 10 μg/ml and 20 μg/ml) (Fig. 1A-

1B). The lowest concentration of (+)-catechin (1.5 μg/ml, 5.168 μM) was used for subsequent studies and this had no effect cell viability (Supplementary Fig. 1A).

To rule out that the (+)-catechin-mediated attenuation of TBHP-induced ROS production was not specific to the THP-1 cell line, comparative analysis was performed on primary HMDM. (+)-catechin has no effect on viability of HMDM (Supplementary Fig. 1B) but it significantly attenuates TBHP-mediated ROS production (Fig. 1C; $p \leq 0.001$). In addition, experiments were extended to primary endothelial and vascular smooth muscle cells given their important roles in atherosclerosis [20]. The TBHP-induced ROS production was attenuated by (+)-catechin in both HUVEC and HASMC ($p \leq 0.001$ and $p = 0.009$ respectively) (Fig. 1D-1E). The viability of HUVECs was not affected by (+)-catechin (Supplementary Fig. 1C). In contrast, there was a negligible but significant reduction in cell viability of about 4% in HASMC ($p = 0.011$; Supplementary Fig. 1D) but this was substantially lower than the reduction in TBHP-induced ROS production in HASMC.

3.2. (+)-catechin modulates macrophage proliferation and MMP activity without affecting apoptosis, pro-inflammatory gene expression, modified LDL uptake and cholesterol efflux from foam cells

Macrophage proliferation plays an important role in atherosclerosis [29]. The effect of (+)-catechin on proliferation of THP-1 macrophages was determined by using crystal violet and bromouridine incorporation assays. A 24 h time point was chosen to ensure sufficient period for determination of changes in cell proliferation. (+)-catechin produced significant reduction in cell proliferation when determined by incorporation of crystal violet (Fig. 2A; $p = 0.029$) or bromouridine (Fig. 2B; $p = 0.034$). The (+)-catechin-mediated inhibition of proliferation was also seen in primary HMDM (Fig. 2C; $p = 0.010$). Such effect on proliferation was specific to monocytes/macrophages and was not observed with HUVEC or HASMC (Supplementary Fig. 2). For HASMC, proliferation was also monitored over a 7-day period and linear regression analysis found no significant differences between the vehicle control

and catechin treatment (data not shown). In contrast to cell proliferation, (+)-catechin had no effect on apoptosis of human macrophages by serum starvation and TNF-α treatment (Fig. 2D).

MMPs produced by macrophages play a critical role in the degradation of ECM [1, 6]. The effects of (+)-catechin on MMP activity was determined at both 3- and 24-h following stimulation of THP-1 macrophages with vehicle or (+)-catechin to delineate both short-term and longer-term actions/effects. (+)-catechin caused significant reduction of MMP activity at both 3 h and 24 h (Fig. 2E-F; p=0.036 and p=0.033 respectively) when compared to the vehicle control. Such inhibitory action was also confirmed in primary HMDM where a significant, but small, reduction was seen at 24 h (Fig. 2G; p=0.005).

Foam cells are formed by an imbalance in cholesterol uptake and cholesterol efflux. In atherogenic conditions, the inflow of cholesterol exceeds outflow and the macrophage becomes a foam cell [20]. The effect of (+)-catechin on both these processes was therefore determined. (+)-catechin had no significant effect on theuptake of DiI-labeled oxLDL (Supplementary Fig. 3A). For cholesterol efflux, macrophages were first converted into foam cells using acetylated LDL, which is avidly taken up by the cells, in the presence of [^{14}C]-cholesterol [20, 21]. The efflux of radioactive cholesterol to apolipoprotein A1 present in HDL particles was then determined and it was not affected by (+)-catechin (Supplementary Fig. 3B).

IFN-γ is a key pro-atherogenic cytokine that induces the expression of MCP-1 and intercellular adhesion molecule-1 (ICAM-1) [30]. The effect of (+)-catechin on IFN-γ induced MCP-1 and ICAM-1 expression in human macrophages was therefore analysed and was not affected by several concentrations of (+)-catechin (Supplementary Fig. 3C-D). We have previously shown that a combination of nutraceuticals that includes catechins attenuates polarization of RAW264.7 macrophages into M1-like phenotype following co-incubation with IFN-γ and lipopolysaccharide (LPS) [24]. The effect of (+)-catechin on M1 macrophage

polarization was therefore investigated. Co-incubation of macrophages with IFN-γ and LPS produced significant increase in expression of five M1 markers [arginase 2 (Arg2), interleukin (IL)-1β, IL-6, inducible nitric oxide synthase (iNOS) and MCP-1] (Supplementary Fig. 3E-I). (+)-catechin did not reduce the expression of any of these markers (Supplementary Fig. 3E-I). However, the expression of Arg2 was induced by (+)-catechin (Supplementary Fig. 3E) indicating that this effect is gene specific.

3.3. (+)-catechin attenuates chemokine-driven monocytic migration and proliferation of these cells

Monocytic migration driven by chemokines such as MCP-1 is a critical early event in atherogenesis [1, 5]. The effect of (+)-catechin on monocytic migration was therefore analysed. (+)-catechin significantly attenuates MCP-1 driven monocytic migration (p=0.049) (Fig. 3A). To investigate whether the effect of (+)-catechin on macrophage proliferation (Fig. 2A-C) also occurred at the level of monocytes, this was assessed on cells grown for 7 days with fresh medium containing either (+)-catechin or vehicle added on days 0, 1, 2, 3 and 4. Cell proliferation showed a significant positive association with time (p≤0.001; adj-R^2=0.57) (Fig. 3B). In addition, cell proliferation was significantly lower in cells receiving (+)-catechin by about 30% (p=0.001) (Fig. 3B). There was no significant effect on interaction between time and treatment type (Fig. 3B).

3.4. (+)-catechin regulates the expression of several atherosclerosis-associated genes in human macrophages

A human Atherosclerosis RT² Profiler PCR Array was used to determine effect of (+)-catechin on gene expression. The chosen time point (3 h) corresponds to inhibition of MMP activity by (+)-catechin (Fig. 2E). A volcano plot for analysis is shown in Fig. 4 and Supplementary Table 4 summarizes the changes in expression of all genes. Expression of four genes was significantly reduced and these code for adhesion protein selectin L (*Sell*; p=0.015), pro-angiogenic vascular endothelial growth factor A (*Vegfa*; p=0.028), LDL

receptor (*Ldlr*; p=0.024) and pro-atherogenic cytokine IFN-γ (*Ifng*; p=0.010). In contrast, the expression of gene encoding peroxisome proliferator-activated receptor-δ, which has anti-atherogenic and anti-inflammatory actions [31], was significantly increased (*Ppard*; p0.001). There was also a trend towards reduced expression of three genes that code for adhesion protein selectin E (*Sele*; p=0.092), platelet-derived growth factor-B (*Pdgfb*; p=0.071) and transcription factor nuclear receptor subfamily 1 group H member 3 (*Nr1h3*; p=0.094), and a trend towards induced expression of one gene, endologin (*Eng*; p=0.087).

3.5. (+)-catechin improves mitochondrial membrane potential in the presence of oxLDL and attenuates migration of HASMC

OxLDL-mediated endothelial cell dysfunction is a critical event in the pathogenesis of atherosclerosis and associated with mitochondrial membrane depolarization [3, 32]. The effect of (+)-catechin on oxLDL-induced mitochondrial depolarization in HUVEC was therefore determined. oxLDL caused significant mitochondrial membrane depolarization (p≤0.001) to a similar extent as the uncoupler FCCP (p≤0.001) (Fig. 5A). However, a significant improvement in oxLDL-induced mitochondrial membrane depolarization was produced by (+)-catechin (p≤0.001).

The migration of vascular smooth muscle cells (SMC) is also an important event in the later stages of atherosclerosis [20]. The effect of (+)-catechin on the migration of HASMC in response to the key growth factor in atherogenesis, PDGF, was therefore determined. The PDGF-mediated migration of these cells was significantly attenuated by (+)-catechin when compared to the vehicle control (p=0.006) (Fig. 5B).

3.6. (+)-catechin produces several favourable changes in plasma parameters associated with atherosclerosis in C57BL/6J mice fed HFD

To evaluate whether the beneficial effects of (+)-catechin *in vitro* extend to atherosclerosis-associated parameters *in vivo* in wild-type mice, experiments were

performed on C57BL/6J mice fed HFD. The approach was based on our recent studies [22, 23] and involved feeding HFD for 3 weeks with daily gavage of vehicle or (+)-catechin hydrate, a water soluble (i.e., avoids use of high concentrations of DMSO in animals) and more cost-effective alternative to (+)-catechin that had similar effects *in vitro* (e.g. inhibition of MCP-1-driven monocytic migration; Supplementary Fig. 4). The concentration of (+)-catechin hydrate used (200 mg/kg/day) was based on published literature on studies on EGCG of 3-week duration [33, 34].

The effect of (+)-catechin hydrate on several plasma parameters is shown in Table 1 and it demonstrates many favorable changes. There was a significant reduction in the levels of TG (p=0.036), TG:total cholesterol ratio (p=0.025) and pro-inflammatory cytokines IL-1β (p=0.032) and IL-2 (p=0.005) (Table 1). There were some determinantal changes such as a significant increase in overall weight gain (p=0.005), weight of total adipose tissue deposits (p=0.002) and total white adipose tissue (p=0.001) together with subcutaneous, gonadal and renal adipose tissue deposits (p≤0.001, p=0.002 and p=0.003 respectively). In addition, there was a significant reduction in the anti-atherogenic cytokine IL-10 (p=0.025; Table 1).

3.7. (+)-catechin regulates the liver expression of several key genes implicated in atherosclerosis in C57BL/6J mice fed HFD

Gene expression changes in the liver have a major impact on metabolism, inflammation and atherosclerosis [20, 22]. The Mouse Atherosclerosis RT² Profiler PCR Array was employed to investigate the effect of (+)-catechin hydrate on the liver expression of 84 key genes implicated in this disease. Fig. 6 shows the volcano plot of global changes in gene expression with Supplementary Table 5 summarising the changes in expression of each gene. Liver expression of 12 genes was significantly altered by (+)-catechin hydrate (Fig. 6). Thus, consistent with (+)-catechin-mediated changes in cell proliferation (Fig. 2), there were significant changes in the expression of several key genes implicated in the regulation of cell proliferation and cell cycle: induced expression of fibroblast growth factor-2

(*Fgf2*; p=0.044), platelet-derived growth factor receptor, β polypeptide (*Pdgfrb*; p=0.002) and kinase insert domain receptor (*Kdr*; p≤0.001). In addition, consistent with the effect on cell migration (Fig. 3A and 5B), the expression of several genes implicated in cell migration and adhesion, ECM and cell-ECM adhesion was affected: increased expression of integrin subunit αX (*Itgax*; p=0.042), *Mmp1a* (p=0.001) and tenascin C (*Tnc*; p=0.025); and decreased expression of integrin subunit α2 (*Itga2*; p=0.043) and fibrinogen β chain (*Fgb*; p=0.028). The expression of *Nr1h3* (codes for anti-atherogenic transcription factor) [35] and *Lpl* (codes for lipoprotein lipase involved in the clearance of circulating lipoproteins) [36] was also induced (p=0.033 and p=0.011 respectively). Other genes whose expression was significantly induced were *Eng* (p=0.011) and lysophospholipase I (*Lypla1*; p=0.043). In addition, there was a trend towards induced expression of *Apoe* (p=0.066) and a trend towards reduced expression of fibrinogen α chain (*Fga*; p=0.056) and heparin-binding EGF-like growth factor (*Hbegf*; p=0.052).

3.8. The effect of (+)-catechin on cell populations in the BM of C57BL/6J mice fed HFD

HFD is associated with changes in the proportion of cell populations in the BM which can then contribute to atherogenesis [37]. Supplementary Fig. 5 shows representative flow plots for gating strategy whereas Fig. 7 indicates changes in the numbers of each class of cells. (+)-catechin hydrate produced significant reduction in the frequency of WBC (p=0.035), MDSC (p=0.029), LSK cells (p=0.001) and CLP (p=0.002). In addition, (+)-catechin hydrate produced a trend towards reduced frequency of LK cells (p=0.065), GMP (p=0.057) and MEP (p=0.057). No significant changes were observed for HPC1 and HPC2, HSC, MPP and CMP (Fig. 7).

3.9. The effect of (+)-catechin on weight gain, weight of organs, and plasma lipids and cytokines in *LDLr*$^{-/-}$ mice fed HFD

Due to the longer duration of 12 weeks (rather than 3) necessary for the formation of established lesions based on our previous studies [20, 21], daily gavage was not used.

Instead, the same dose of (+)-catechin hydrate (200 mg/kg/day) was mixed directly into HFD, to mitigate any adverse effects that may arise from long-term daily gavage compounding study results. There were no significant changes in any adiposity-associated parameters (Table 2). Additionally, although there was a significant increase in plasma total cholesterol (p=0.013; Table 2), no significant detrimental changes in any of the associated lipid ratios were identified. However, there was a trend of decrease in TG levels (p=0.077; Table 2). Furthermore, there was a reduction in plasma levels of IL-5 (p=0.048; Table 2), whilst the levels of IFN-γ were increased (p=0.048; Table 2). Additionally, there was trend towards increase in the levels of IL-1β (p=0.093; Table 2) and IL-6 (p=0.066; Table 2). There were no changes in any other plasma cytokine levels.

3.10. (+)-catechin attenuates plaque burden without affecting the lipid content

Sections of the aortic root at the three valve cusps were stained for neutral lipids with ORO to assess atherosclerotic plaque development and burden. From the images of stained sections, various parameters were calculated following image analysis; plaque lipid content, plaque content within vessel, degree of occlusion within the lumen, and plaque and vessel size (Fig. 8). The catechin group had reduced plaque content (p=0.048; Fig. 8C), occlusion (p=0.049; Fig. 8D) and plaque size (p=0.067; Fig. 8E) compared to the control group without an effect on the lipid content (Fig. 8B), which is consistent with no effects in foam cell formation parameters *in vitro* (Supplementary Fig. 3) There was also no significant change in vessel size (i.e., vessel remodelling) (Fig. 8F).

3.11. (+)-catechin reduces the infiltration of macrophages to developing atherosclerotic plaques with no effect on T cells

Immunofluorescence staining was used to detect the presence of macrophages and T cells (Fig. 9). Consistent with decreased chemokine-driven monocytic migration and monocyte/macrophage proliferation *in vitro* (Figs. 2-3), the catechin group had marked reduction in the proportion of MOMA-2^+ macrophages (p≤0.001; Fig. 9B). However, there

was no significant difference in the proportion of plaque $CD3^+$ T cells between the two groups (Fig. 9C).

3.12. (+)-catechin promotes plaque SMC and collagen content without affecting plaque necrosis

For assessment of plaque necrosis and markers of stability, acellular areas within atherosclerotic plaque were quantified, and plaque collagen (using van Gieson's staining) and αSMA^+ SMC (using immunofluorescence staining) content were measured (Fig. 10). Plaque stability markers were calculated using combined data from immunohistochemical and immunofluorescence staining as (VSMC area + collagen area)/(macrophage area + lipid area). The catechin group had significantly increased collagen content (p=0.033) and αSMA^+ SMCs (p=0.038) in the plaque compared to the control group (Fig. 10A-D). There was, hence, a significant increase in plaque stability index by 58.87% (p=0.026), although no significant differences in plaque necrosis were found between the two groups (Fig. 10E-F).

3.13. The effect of (+)-catechin on cell populations in the BM of *LDLr*$^{-/-}$ mice

Supplementary Fig. 5 shows the gating strategy whilst Supplementary Fig. 6 indicates changes in the numbers of each class of cells. (+)-catechin hydrate produced a decrease in the frequency of CMP (p=0.016). No significant changes were observed for total WBC, MDSC, LSK, HPCs, HSC, MPP, LK, GMP, MEP and CLP (Supplementary Fig. 6).

4. Discussion

Despite a study of 34,492 participants demonstrating a strong inverse association between the intake of (+)-catechin and coronary heart disease [10], the mechanisms underlying such beneficial actions are poorly understood and therefore formed the focus of the present study. We show that (+)-catechin attenuates several pro-atherogenic processes *in vitro* in human macrophages, endothelial cells and vascular smooth muscle cells without

demonstrating any detrimental effects (Figs. 1-5). The beneficial actions of (+)-catechin also extended *in vivo* to C57BL/6J mice fed HFD for 3-weeks (Table 1 and Fig. 6). In *LDLr*$^{-/-}$ mice fed HFD for 12-weeks, (+)-catechin attenuated atherosclerotic plaque development and progression (Fig. 8 and 9) without affecting lipid content; increased markers of plaque stability (Fig. 10) without affecting necrosis; and reduced levels of CMP in BM (Supplementary Fig. 6). Taken together, these studies provide novel insights into the athero-protective actions of (+)-catechin and the potential underlying mechanisms.

Gene expression profiling of human macrophages showed significant reduction in the expression of four genes (*Sell*, *Vegfa*, *Ldlr* and *Ifng*) and induced expression of *Ppard* (Fig. 4). In addition, there was a trend towards reduced expression of *Sele*, *Pdgfb* and *Nr1h3* and increased expression of *Eng* (Fig. 4). IFN-γ is potentially a master regulator of atherosclerosis and this cytokine also regulates the expression of 30% of macrophage transcriptome [38]. Macrophages play pivotal roles in atherosclerosis and this effect of (+)-catechin therefore represents a key anti-atherogenic action. Adhesion proteins, such as SELL and SELE, are involved in the recruitment of leukocytes to the activated endothelium [38], and their reduced expression is consistent with the (+)-catechin-mediated decrease in monocytic migration (Fig. 3A). Although previous studies on SELL in mouse model systems have not produced consistent results [39, 40], reduced protein levels were observed in obese individuals following 4-weeks of flavanol-rich cocoa consumption [41]. On the other hand, deficiency of SELE is associated with smaller atherosclerotic lesions in mouse model systems [42]. VEGFA is a key promoter of angiogenesis but also modulates cell migration and proliferation, including macrophages [39]. Studies in *ApoE*$^{-/-}$ mice have also shown VEGFA to enhance atherosclerosis development [44, 45]. The (+)-catechin-mediated reduction in *Vegfa* expression is also consistent with decreased monocytic migration and macrophage proliferation. Indeed, these changes correlate with marked reduction in plaque macrophage content (Fig. 9B) in *LDLr*$^{-/-}$ mice, which may be a consequence of both reduced monocyte recruitment to the endothelium and subsequent infiltration to the intima, along with

decreased local macrophage proliferation. There was no difference in plaque lipid content (Fig. 8B), correlating to lack of change in macrophage foam cell formation parameters (Supplementary Fig. 3), thereby suggesting key anti-inflammatory effects of (+)-catechin *in vivo*. (+)-catechin also increased the expression of *Ppard*, a key regulator of anti-atherogenic and anti-inflammatory gene expression programmes in macrophages [31]. Increased synthesis and activity of MMPs are responsible for plaque destabilization [6, 46]. (+)-catechin reduced MMP activity (Fig. 2E-G) and this correlates with reduced expression of IFN-γ (Fig. 4), which is known to induce MMP activities [38]. Fittingly, *LDLr*$^{-/-}$ mice receiving (+)-catechin supplemented HFD had greater levels of αSMA^{+} cells and collagen within the plaque, suggesting greater presence/maintenance of plaque-stabilizing fibrous cap, possibly via protection against MMP-mediated degradation of constituent ECM proteins (Fig. 10F). Reduced *Eng* expression is associated with nitric oxide synthase uncoupling and subsequent ROS production [47]. Thus, (+)-catechin-mediated increased expression of the *Eng* gene (Figs. 4 and 6) is potentially one contributing factors for its antioxidant actions. It should, however, be noted that not all gene expression changes are anti-atherogenic. Thus, the reduced expression of the *Ldlr* gene could potentially be pro-atherogenic as the receptor aids in the clearance of circulating LDL, and thereby plaque formation.

Plasma TG levels are indicators of VLDL, chylomicron remnants and TG-rich lipoproteins, all of which are able of exacerbating atherosclerosis [48]. In C57BL/6J mice, (+)-catechin hydrate reduced plasma TG levels (Table 1) with a trend towards decrease in *LDLr*$^{-/-}$ mice (Table 2) and this could be due to increased liver expression of *Lpl* and *Nr1h3* (Fig. 6). LPL is involved in the clearance of circulating chylomicrons and VLDL by catalysing their hydrolysis into non-esterified fatty acids and 2-monoacyl glycerol for tissue utilization [36]. In addition, NR1H3 reduces the production of chylomicrons via a mechanism dependent on apical localisation of SR-B1 [49] and also inhibits insulin-mediated VLDL secretion [50]. Increased expression of *Nr1h3* is also likely to contribute to reduced plasma levels of IL-1β and IL-2 (Table 1) given its anti-inflammatory actions [35]. Both IL-1β and IL-2

are pro-atherogenic and circulating levels of IL-1β are indicative of NLR family pyrin domain containing 3 (NLRP3) inflammasome activation associated with atherosclerotic disease progression and plaque instability [38].

The liver expression of 12 genes was significantly changed by (+)-catechin hydrate with an additional three showing trends of altered expression (Fig. 6). Several of these changes are anti-atherogenic. For example, LPL is involved in the clearance of plasma lipoproteins [36] and NR1H3 initiates an anti-atherogenic and anti-inflammatory gene expression program [35]. The expression of *Eng* is associated with plaque stabilization and reduced ROS production [51]. Integrin signalling plays important roles in atherosclerosis, including in platelet activation and leukocyte homing [52], so reduced expression of *Itga2* is potentially beneficial. The expression of *Apoe* was increased and the corresponding protein is known to have anti-atherogenic and anti-inflammatory properties [53]. Decreased expression of *Fga* and *Fgb* is also beneficial as increased plasma fibrinogen levels are linked to elevated risk for myocardial infarction and coronary artery disease [54]. Tenascin-C has been implicated in regulating cell adhesion, inflammation and tissue modelling and its deficiency enhances atherogenesis in *ApoE*$^{-/-}$ mice via increased cell infiltration and intraplaque haemorrhage [55]. Thus, the increased expression of *Tnc* gene is also athero-protective.

(+)-catechin hydrate produced several beneficial changes in the population of cells within the BM (Fig. 7). For example, the numbers of WBC, which are positively correlated with inflammation and atherosclerosis [56], was attenuated. HFD increases LSK, CLP and GMP populations [57, 58] and these were reduced by (+)-catechin hydrate in HFD-fed C57BL/6J mice, whilst only CMP levels were reduced in HFD-fed *LDLr*$^{-/-}$ mice (Supplementary Fig. 6).

In conclusion, this study provides novel insights into the molecular mechanisms underlying the cardioprotective actions of (+)-catechin. The flavanoid attenuates several pro-

atherogenic processes *in vitro* and *in vivo*. Whilst the *in vitro* studies provided novel mechanistic insights, they have to be interpreted with caution because of the high, potentially supraphysiological concentration used, despite being based on initial dose-response experiments, and simplification of processes that occur *in vivo* where interactions between multiple cell types and their environment are involved. The most important *in vivo* finding was that (+)-catechin attenuates atherosclerosis development and progression in the *LDLr*$^{-/-}$ mouse model and increases markers of plaque stability. These studies therefore highlight the potential of (+)-catechin for the prevention, and possibly treatment, of atherosclerosis. The concentration of (+)-catechin used for *in vivo* studies (200 mg/kg/day), which was based on published literature, equates to 16.2 mg/kg/day according to guide for dose conversion between animals and human [59, 60]. Future work should carry out dose-response experiments together with investigation of the efficacy of (+)-catechin on regression of existing/established atherosclerotic plaques in mouse model systems, and on CVD burden and associated risk factors in clinical trials.

Acknowledgements

We acknowledge funding from the British Heart Foundation (grants FS/17/75/33257 and PG/16/25/32097). JWEM was funded by a joint PhD studentship between the School of Biosciences and Cultech Limited and NA was funded by a PhD studentship from the Kingdom of Saudi Arabia.

Conflict of Interest

This study was supported in part by Cultech Ltd. DRM and SFP are employees of Cultech Ltd. JWEM PhD was funded by a joint PhD studentship between the School of Biosciences and Cultech Limited.

Author Contributions

Y-HC, JWEM, JOW, TRH, SFP, DRM, NPR and DPR designed experiments, which were performed by Y-HC, JWEM, JOW, NF and NA. Data analysis was carried out by Y-HC, JWEM, JOW, NF, NA and JBM-G. Y-HC, JWEM, JOW and JBM-G prepared the figures and Y-HC and DPR wrote manuscript. All authors contributed to review of manuscript.

5. References

[1] Moss, J. W. E., Ramji, D. P., Nutraceutical therapies for atherosclerosis. *Nat Rev Cardiol* 2016, *13*, 513-532.

[2] O'Morain, V. L., Ramji, D. P., The potential of probiotics in the prevention and treatment of atherosclerosis. *Mol Nutr Food Res* 2020, *64*, e1900797.

[3] García-Cardeña, G., Gimbrone Jr, M. D., Endothelial cell dysfunction and the pathobiology of atherosclerosis. *Circ Res* 2016, *118*, 620.

[4] Poznyak, A. V., Nikiforov, N. G., Markin, A. M., Kashiskikh, D. A., Myasoedova, V. A., Gerasimova, E. V., Orekhov, A. N. Overview of oxLDL and its impact on cardiovascular health. *Front Pharmacol* 2020, *11*, 613780.

[5] Gencer, S., Evans, B. R., van der Vorst, E. P. C., Döring, Y., Weber, C. Inflammatory chemokines in atherosclerosis. *Cells* 2021, *10*, 226.

[6] Johnson JL. Metalloproteinases in atherosclerosis. *Eur J Pharmacol* 2017, *816*, 93.

[7] Vesnina, A., Prosekov, A., Atuchin, V., Minina, V., Ponasenko, A., Tackling atherosclerosis via selected nutrition. *Int J Mol Sci* 2022, *23*, 8233.

[8] Vesnina, A., Prosekov, A., Kozlova, O., Atuchin, V., Genes and eating preferences, their roles in personalized nutrition. *Genes (Basel)* 2020, *11*, 357.

[9] Mangels, D. R., Mohler, E. R., Catechins as potential mediators of cardiovascular health. *Arterioscler Thromb Vasc Biol* 2017, *37*, 757-763.

[10] Arts, I. C., Jacobs, D. R., Harnack, L. J., Gross, M., Folsom, A. R., Dietary catechins in relation to coronary heart disease death among postmenopausal women. *Epidemiology* 2001, *12*, 668-675.

[11] Sesso, H. D., Manson, J. E., Aragaki, A. K., Rist, P. M.*, et al.*, Effect of cocoa flavanol supplementation for prevention of cardiovascular disease events: The COSMOS randomized clinical trial. *Am J Clin Nutr* 2022, *115*, 1490-1500.

[12] Morrison, M., van der Heijden, R., Heeringa, P., Kaijzel, E.*, et al.*, Epicatechin attenuates atherosclerosis and exerts anti-inflammatory effects on diet-induced human-CRP and NFκB *in vivo*. *Atherosclerosis* 2014, *233*, 149-156.

[13] Yin, J., Huang, F., Yi, Y., Yin, L., Peng, D., EGCG attenuates atherosclerosis through the Jagged-1/Notch pathway. *Int J Mol Med* 2016, *37*, 398-406.

[14] Cai, Y., Kurita-Ochiai, T., Hashizume, T., Yamamoto, M., Green tea epigallocatechin-3-gallate attenuates *Porphyromonas gingivalis*-induced atherosclerosis. *Pathog Dis* 2013, *67*, 76-83.

[15] Chyu, K. Y., Babbidge, S. M., Zhao, X., Dandillaya, R.*, et al.*, Differential effects of green tea-derived catechin on developing versus established atherosclerosis in apolipoprotein E-null mice. *Circulation* 2004, *109*, 2448-2453.

[16] Miura, Y., Chiba, T., Tomita, I., Koizumi, H.*, et al.*, Tea catechins prevent the development of atherosclerosis in apoprotein E-deficient mice. *J Nutr* 2001, *131*, 27-32.

[17] Auclair, S., Milenkovic, D., Besson, C., Chauvet, S.*, et al.*, Catechin reduces atherosclerotic lesion development in apoE-deficient mice: a transcriptomic study. *Atherosclerosis* 2009, *204*, e21-27.

[18] Liu, L., Nagai, I., Gao, Y., Matsushima, Y., *et al.*, Effects of catechins and caffeine on the development of atherosclerosis in mice. *Biosci Biotechnol Biochem* 2017, *81*, 1948-1955.

[19] Ramji, D. P., Chan, Y. H., Alahmadi, A., Alotibi, R., Alshehri, N., Survey of approaches for investigation of atherosclerosis *in vivo*. *Methods Mol Biol* 2022, *2419*, 57-72.

[20] O'Morain, V. L., Chan, Y. H., Williams, J. O., Alotibi, R., *et al.*, The Lab4P consortium of probiotics attenuates atherosclerosis in LDL receptor deficient mice fed a high fat diet and causes plaque stabilization by inhibiting inflammation and several pro-atherogenic processes. *Mol Nutr Food Res* 2021, *65*, e2100214.

[21] Al-Ahmadi, W., Webberley, T. S., Joseph, A., Harris, F., *et al.*, Pro-atherogenic actions of signal transducer and activator of transcription 1 serine 727 phosphorylation in LDL receptor deficient mice via modulation of plaque inflammation. *FASEB J* 2021, *35*, e21892.

[22] Moss, J. W. E., Williams, J. O., Al-Ahmadi, W., O'Morain, V., *et al.*, Protective effects of a unique combination of nutritionally active ingredients on risk factors and gene expression associated with atherosclerosis in C57BL/6J mice fed a high fat diet. *Food Funct* 2021, *12*, 3657-3671.

[23] Michael, D. R., Davies, T. S., Moss, J. W. E., Calvente, D. L., *et al.*, The anti-cholesterolaemic effect of a consortium of probiotics: An acute study in C57BL/6J mice. *Sci Rep* 2017, *7*, 2883.

[24] Moss, J. W.E, Davies, T. S., Garaiova, I., Plummer, S. F., *et al.*, A unique combination of nutritionally active ingredients can prevent several key processes associated with atherosclerosis *in vitro*. *PLoS One* 2016, *11*, e0151057.

[25] Chan, Y. H., Alahmadi, A., Alotibi, R., Ramji, D. P., Evaluation of plaque burden and lipid content in atherosclerotic plaques. *Methods Mol Biol* 2022, *2419*, 481-496.

[26] Chan, Y. H., Alotibi, R., Alahmadi, A., Ramji, D. P., Monitoring cellularity and expression of key markers in atherosclerotic plaques. *Methods Mol Biol* 2022, *2419*, 497-506.

[27] Solanki, S., Dube, P. R., Birnbaumer, L., Vazquez, G., Reduced necrosis and content of apoptotic M1 macrophages in advanced atherosclerotic plaques of mice with macrophage-specific loss of Trpc3. *Sci Rep* 2017, *7*, 42526.

[28] Liu, X., Li, J., Liao, J., Wang, H.*, et al.*, Gpihbp1 deficiency accelerates atherosclerosis and plaque instability in diabetic Ldlr(-/-) mice. *Atherosclerosis* 2019, *282*, 100-109.

[29] Robbins, C. S., Hilgendorf, I., Weber, G. F., Theurl, I.*, et al.*, Local proliferation dominates lesional macrophage accumulation in atherosclerosis. *Nat Med* 2013, *19*, 1166-1172.

[30] Gallagher, H., Williams, J. O., Ferekidis, N., Ismail, A.*, et al.*, Dihomo-γ-linolenic acid inhibits several key cellular processes associated with atherosclerosis. *Biochim Biophys Acta* 2019, *1865*, 2538-2550.

[31] Cheang, W. S., Tian, X. Y., Wong, W. T., Huang, Y., The peroxisome proliferator-activated receptors in cardiovascular diseases: experimental benefits and clinical challenges. *Br J Pharmacol* 2015, *172*, 5512-5522.

[32] Hort, M. A., Straliotto, M. R., de Oliveira, J., Amoêdo, N. D.*, et al.*, Diphenyl diselenide protects endothelial cells against oxidized low density lipoprotein-induced injury: Involvement of mitochondrial function. *Biochimie* 2014, *105*, 172-181.

[33] Potenza, M. A., Marasciulo, F. L., Tarquinio, M., Tiravanti, E.*, et al.*, EGCG, a green tea polyphenol, improves endothelial function and insulin sensitivity, reduces

blood pressure, and protects against myocardial I/R injury in SHR. *Am J Physiol Endocrinol Metab* 2007, *292*, E1378-1387.

[34] Potenza, M. A., Montagnani, M., Nacci, C., De Salvia, M. A., Chronic treatment with epigallocatechin gallate reduces motor hyperactivity and affects *in vitro* tested intestinal motility of spontaneously hypertensive rats. *Food Nutr Res* 2016, *60*, 28373.

[35] Michael, D. R., Ashlin, T. G., Buckley, M. L., Ramji, D. P., Liver X receptors, atherosclerosis and inflammation. *Current Atherosclerosis Reports* 2012, *14*, 284-293.

[36] Mead, J. R., Irvine, S. A., Ramji, D. P., Lipoprotein lipase: structure, function, regulation, and role in disease. *J Mol Med* 2002, *80*, 753-769.

[37] Nahrendorf, M., Swirski, F. K., Lifestyle effects on hematopoiesis and atherosclerosis. *Circ Res* 2015, *116*, 884-894.

[38] Ramji, D. P., Davies, T. S., Cytokines in atherosclerosis: Key players in all stages of disease and promising therapeutic targets. *Cytokine Growth Factor Rev* 2015, *26*, 673-685.

[39] Galkina, E., Kadl, A., Sanders, J., Varughese, D.*, et al.*, Lymphocyte recruitment into the aortic wall before and during development of atherosclerosis is partially L-selectin dependent. *J Exp Med* 2006, *203*, 1273-1282.

[40] Gjurich, B. N., Taghavie-Moghadam, P. L., Ley, K., Galkina, E. V., L-selectin deficiency decreases aortic B1a and Breg subsets and promotes atherosclerosis. *Thromb Haemost* 2014, *112*, 803-811.

[41] McFarlin, B. K., Venable, A. S., Henning, A. L., Prado, E. A.*, et al.*, Natural cocoa consumption: Potential to reduce atherogenic factors? *J Nutr Biochem* 2015, *26*, 626-632.

[42] Collins, R. G., Velji, R., Guevara, N. V., Hicks, M. J., *et al.*, P-Selectin or intercellular adhesion molecule (ICAM)-1 deficiency substantially protects against atherosclerosis in apolipoprotein E-deficient mice. *J Exp Med* 2000, *191*, 189-194.

[43] Smith, G. A., Fearnley, G. W., Harrison, M. A., Tomlinson, D. C., *et al.*, Vascular endothelial growth factors: multitasking functionality in metabolism, health and disease. *J Inherit Metab Dis* 2015, *38*, 753-763.

[44] Heinonen, S. E., Kivelä, A. M., Huusko, J., Dijkstra, M. H., *et al.*, The effects of VEGF-A on atherosclerosis, lipoprotein profile, and lipoprotein lipase in hyperlipidaemic mouse models. *Cardiovasc Res* 2013, *99*, 716-723.

[45] Celletti, F. L., Waugh, J. M., Amabile, P. G., Brendolan, A., *et al.*, Vascular endothelial growth factor enhances atherosclerotic plaque progression. *Nat Med* 2001, *7*, 425-429.

[46] Buckley, M. L., Ramji, D. P., The influence of dysfunctional signaling and lipid homeostasis in mediating the inflammatory responses during atherosclerosis. *Biochim Biophys Acta* 2015, *1852*, 1498-1510.

[47] Belik, J., Jerkic, M., McIntyre, B. A., Pan, J., *et al.*, Age-dependent endothelial nitric oxide synthase uncoupling in pulmonary arteries of endoglin heterozygous mice. *Am J Physiol Lung Cell Mol Physiol* 2009, *297*, L1170-1178.

[48] Talayero, B. G., Sacks, F. M., The role of triglycerides in atherosclerosis. *Curr Cardiol Rep* 2011, *13*, 544-552.

[49] Briand, O., Touche, V., Colin, S., Brufau, G., *et al.*, Liver X receptor regulates triglyceride absorption through intestinal down-regulation of scavenger receptor class B, type 1. *Gastroenterology* 2016, *150*, 650-658.

[50] Grefhorst, A., Parks, E. J., Reduced insulin-mediated inhibition of VLDL secretion upon pharmacological activation of the liver X receptor in mice. *J Lipid Res* 2009, *50*, 1374-1383.

[51] Nachtigal, P., Zemankova Vecerova, L., Rathouska, J., Strasky, Z., The role of endoglin in atherosclerosis. *Atherosclerosis* 2012, *224*, 4-11.

[52] Finney, A. C., Stokes, K. Y., Pattillo, C. B., Orr, A. W., Integrin signaling in atherosclerosis. *Cell Mol Life Sci* 2017, *74*, 2263-2282.

[53] Greenow, K., Pearce, N. J., Ramji, D. P., The key role of apolipoprotein E in atherosclerosis. *J Mol Med* 2005, *83*, 329-342.

[54] Reinhart, W. H., Fibrinogen--marker or mediator of vascular disease? *Vasc Med* 2003, *8*, 211-216.

[55] Wang, L., Wang, W., Shah, P. K., Song, L.*, et al.*, Deletion of tenascin-C gene exacerbates atherosclerosis and induces intraplaque hemorrhage in Apo-E-deficient mice. *Cardiovasc Pathol* 2012, *21*, 398-413.

[56] Ates, A. H., Canpolat, U., Yorgun, H., Kaya, E. B.*, et al.*, Total white blood cell count is associated with the presence, severity and extent of coronary atherosclerosis detected by dual-source multislice computed tomographic coronary angiography. *Cardiol J* 2011, *18*, 371-377.

[57] Ma, X., Feng, Y., Hypercholesterolemia tunes hematopoietic stem/progenitor cells for inflammation and atherosclerosis. *Int J Mol Med* 2016, *17*, 1162.

[58] Feng, Y., Schouteden, S., Geenens, R., Van Duppen, V.*, et al.*, Hematopoietic stem/progenitor cell proliferation and differentiation is differentially regulated by high-density and low-density lipoproteins in mice. *PLoS One* 2012, *7*, e47286.

[59] Nair, A. B., Jacob, S., A simple practice guide for dose conversion between animals and human. *J Basic Clin Pharm* 2016, *7*, 27-31.

[60] Reagan-Shaw, S., Nihal, M., Ahmad, N., Dose translation from animal to human studies revisited. *FASEB J* 2008, *22*, 659-661.

Figure Legends

Figure 1. (+)-catechin attenuates TBHP-induced ROS production in human monocytes, macrophages, endothelial cells, and smooth muscle cells

ROS production was assessed in THP-1 monocytes and macrophages (A and B respectively), HMDM (C), HUVEC (D) and HASMC (E) incubated for 3 h in absence (-) or presence of 50 μM TBHP (+) with vehicle or indicated concentration of (+)-catechin (A-B) or 1.5 μg/ml (+)-catechin (C-E). ROS production was determined as in Materials and Methods with values from cells treated with vehicle alone (Vehicle-) arbitrarily assigned as 1. Data (mean ± SEM) are from three (A-C) or four (D-E) independent experiments and statistical analysis was performed using one-way ANOVA with Tukey's (A, E) or Games-Howell (B-D) post-hoc analysis (log-transformed data were used for A-B; * $p \leq 0.05$; ** $p \leq 0.01$ and *** $p \leq 0.001$).

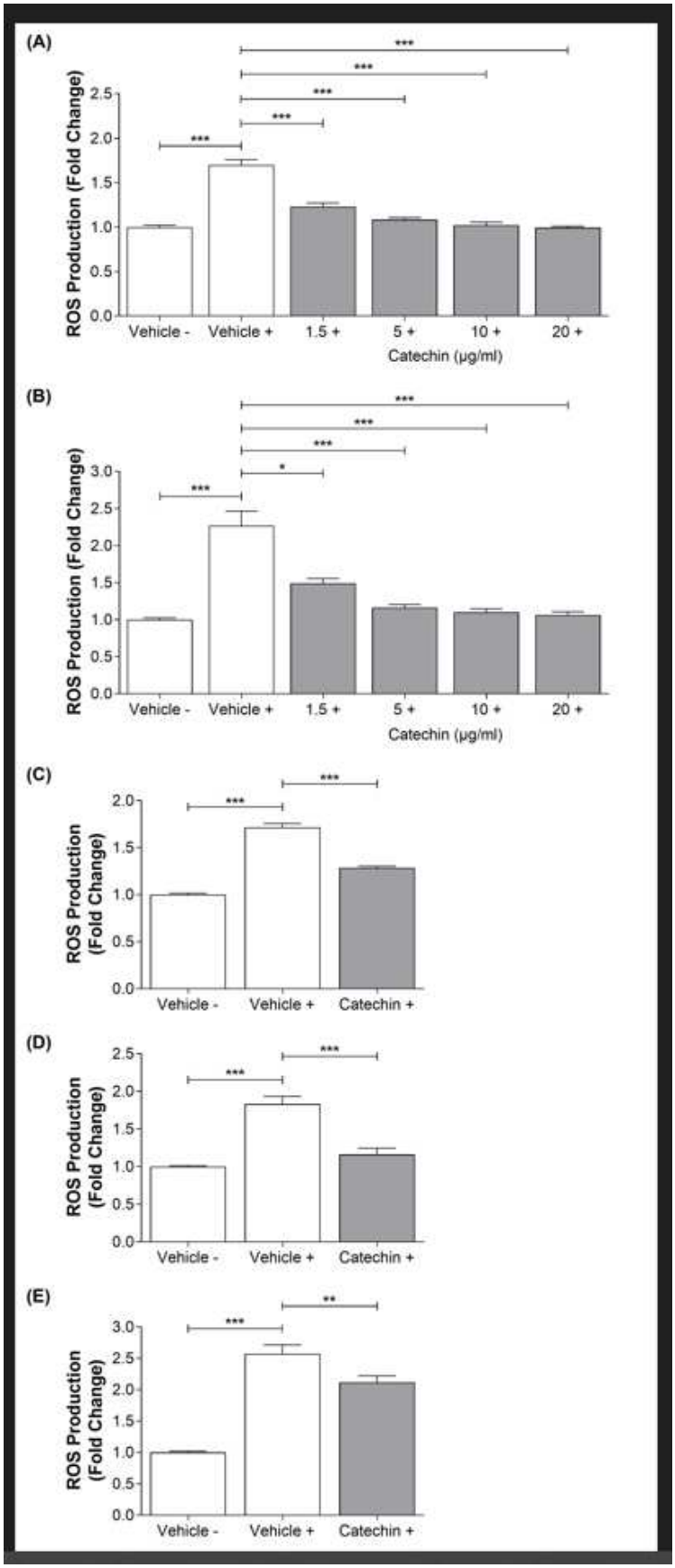

Figure 2. (+)-catechin attenuates human macrophage proliferation and MMP activity

For cell proliferation and MMP activity, THP-1 macrophages (A-B, D-F) or HMDM (C, G) were incubated for 3 h (E) or 24 h (A-C, F-G) with vehicle or 1.5 µg/ml (+)-Catechin. For cell apoptosis (D), THP-1 macrophages were incubated for 3 h with vehicle alone (Vehicle) or in serum-free medium with 100 ng/ml TNF-α to induce apoptosis (+) with vehicle or 1.5 µg/ml (+)-Catechin. Assays were carried out as in Materials and Methods (crystal violet for A and C, bromouridine for B) with values from cells treated with vehicle alone arbitrarily assigned as 1. Data (mean ± SEM) are from three (A, D-F), four (B) or five (C, G) independent experiments and statistical analysis was performed using an unpaired Student's t test (A-C, E-G) or one-way ANOVA with Dunnett post-hoc analysis (D) (* $\leq p$ 0.05; ** $p \leq 0.01$ and $p \leq 0.001$).

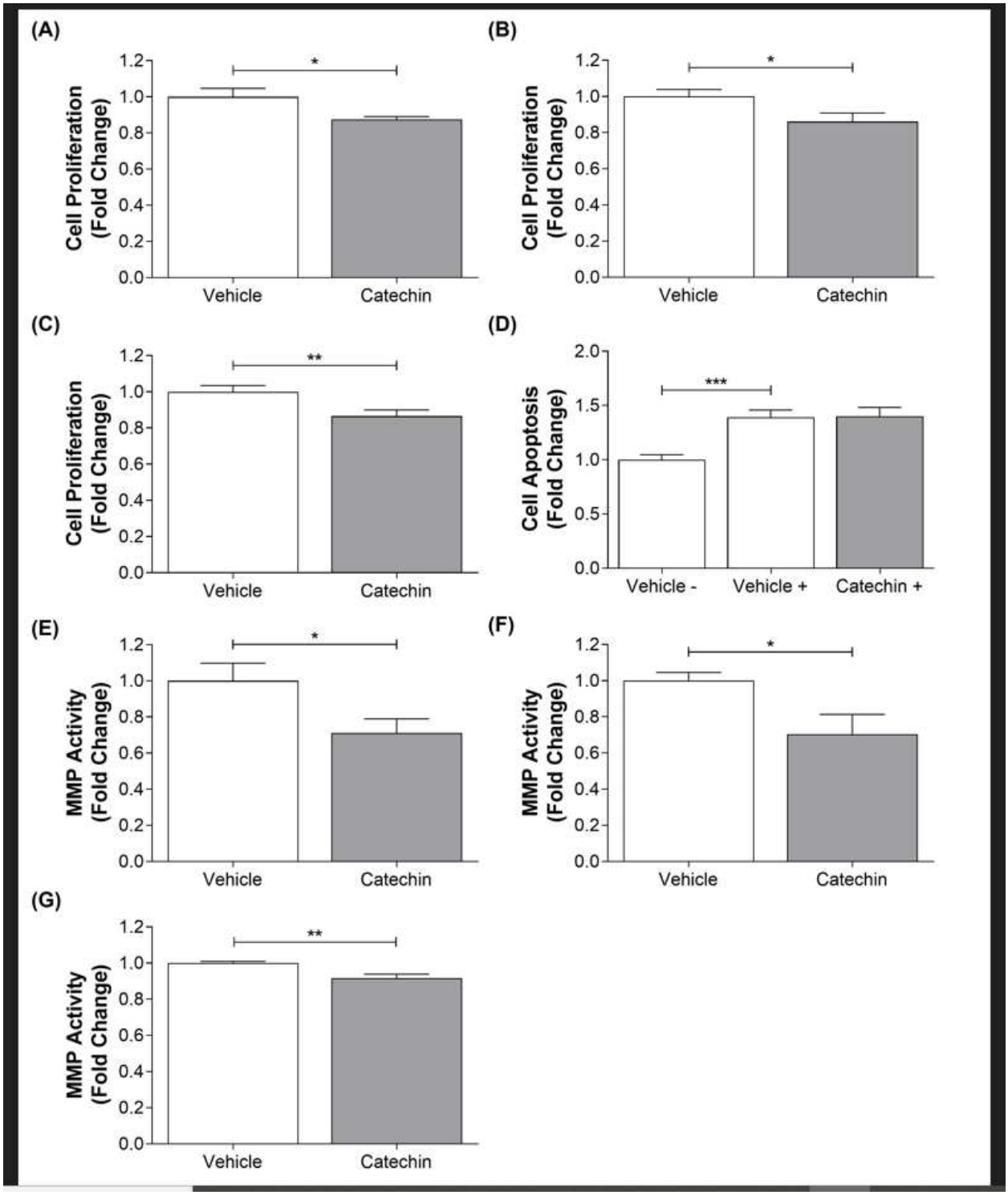

Figure 3. (+)-catechin inhibits MCP-1 driven monocytic migration and proliferation of these cells

(A) Migration assays were performed with THP-1 monocytes incubated for 3 h with MCP-1 (+, 20 ng/ml) in the presence of vehicle or 1.5 µg/ml (+)-

Catechin. Cells incubated with vehicle in the absence MCP-1 were included for comparative purposes (Vehicle-). Monocyte migration was determined by cell counting and expressed as a percentage of total input cells. Graph displays percentage migration (mean +/- SEM), with values from Vehicle+ arbitrarily assigned as 1. Statistical analysis was performed using one-way ANOVA with Dunnett post-hoc analysis (* $p \leq 0.05$ and *** $p \leq 0.001$). (B) Cell proliferation was assessed in THP-1 monocytes either treated with vehicle (dashed line) or (+)-catechin (1.5 µg/ml; solid line) for 7 days by cell counting. Values from vehicle treated cells on day 0 were given an arbitrary value of 1 and all other data are normalised to this. The prediction of average monocyte proliferation fold change as calculated by a generalised linear model with Gaussian error distribution and log link function is displayed ± SEM from three independent experiments.

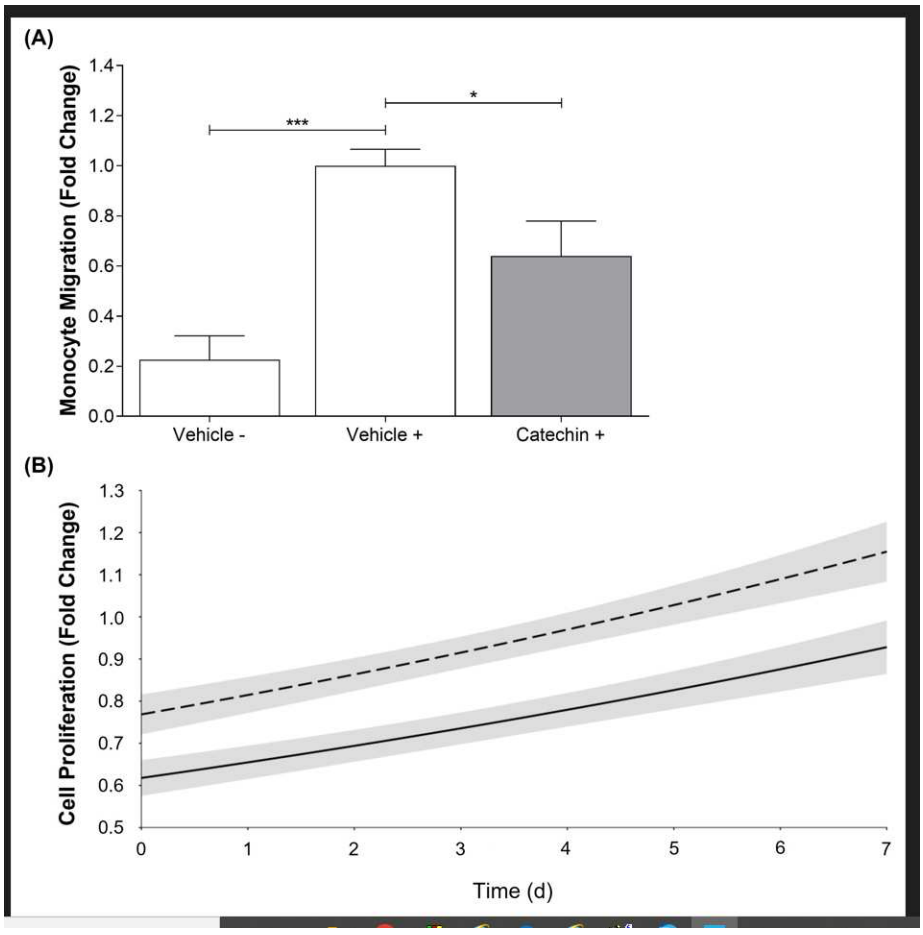

Figure 4. Volcano plot showing global gene expression changes by (+)-catechin in human macrophages

Transcript levels of 84 genes were assessed in human THP-1 macrophages treated with either vehicle or (+)-catechin (1.5 μg/ml) for 3 h. The log fold change treated cells versus vehicle control is represented on x-axis. The y-axis shows the -log10 of p value. A p value of 0.05 (dashed line) is indicated. Significantly altered gene expressions are in indicated by filled triangle and non-significant trends towards change (p≤0.1) are indicated by filled square. *Abbreviations*: *ENG*, endoglin; *IFNG*, interferon-γ; *LDLR*, LDL receptor; *NR1H3*, nuclear receptor subfamily 1 group H member 3; *PDGFB*, platelet-derived growth factor subunit B; *PPARD*, peroxisome proliferator activator receptor-δ; *SELE*, selectin E; *SELL*, selectin L; *VEGFA*, vascular endothelial growth factor A

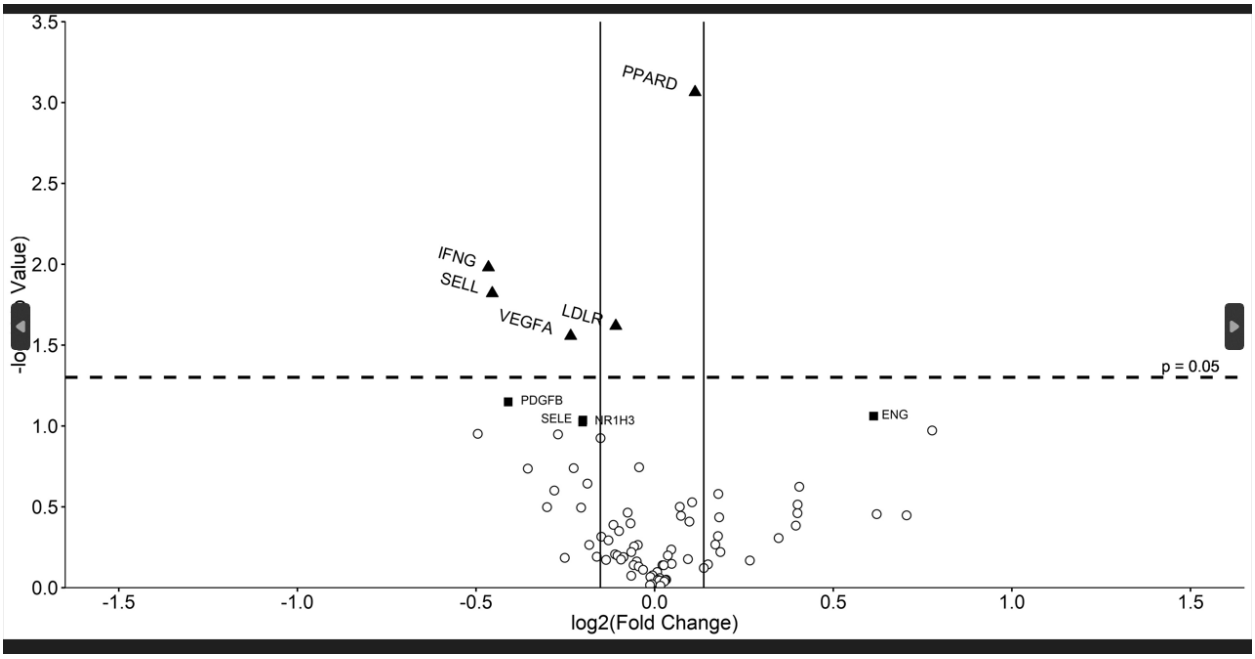

Figure 5. (+)-catechin attenuates oxLDL-induced endothelial cell membrane polarization and growth factor-mediated migration of smooth muscle cells

(A) HUVEC were treated for 24 h with vehicle alone or with oxLDL (100 μg/ml) in the presence of vehicle or 1.5 μg/ml (+)-catechin as indicated. Cells incubated with vehicle and FCCP (100 μM) were also included for

comparative purposes. Mitochondrial membrane potential was determined as in Materials and Methods. (B) HASMC migration was performed as described in Materials and Methods with cells incubated with PDGF (+; 20 ng/ml) in presence of vehicle or 1.5 μg/ml (+)-catechin. Cells incubated with vehicle alone without PDGF (-) were also included for comparison. The results are expressed as fold change of migrated cells determined in five fields of view in relation to vehicle+ control (arbitrarily assigned as 1). Data (mean ± SEM) are from three (A) or four (B) independent experiments. Statistical analysis was performed using one-way ANOVA with Tukey's post-hoc analysis (*, $p \leq 0.05$ and ***, $p \leq 0.001$).

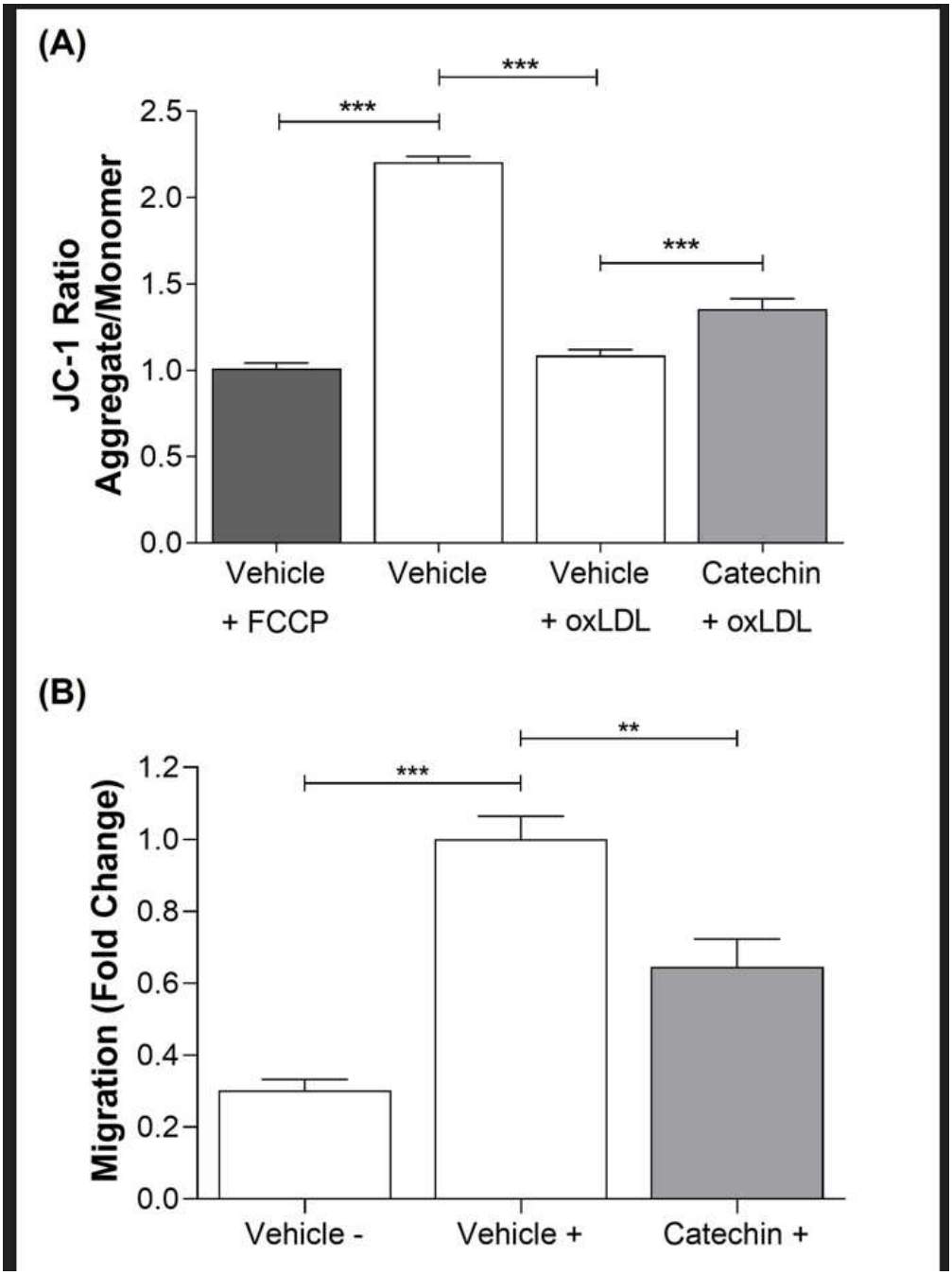

Figure 6. Volcano plot showing global gene expression changes in the liver of mice fed HFD and treated with (+)-catechin hydrate or vehicle

Transcript levels were assessed in the livers of mice after 21 days of HFD and treatment with either vehicle or (+)-catechin hydrate. The log fold change following treatment vs the vehicle control is represented on the x-axis. The y-axis shows -log10 of p value (a *p* value of 0.05 is indicated by a dashed line). Significantly altered gene expressions are

indicated by filled triangle and non-significant trends of change ($p \leq 0.1$) are shown by a filled square. *Abbreviations*: *APOE*, apolipoprotein E; *ENG*, endoglin; *FGA*, fibrinogen α chain; *FGB*, fibrinogen β chain; *FGF2*, fibroblast growth factor-2; *HBEGF*, heparin-binding EGF-like growth factor; *ITAG2*, integrin subunit α2; *ITGAX*, integrin subunit αX; *KDR*, kinase insert domain receptor; *LPL*, lipoprotein lipase; *LYPLA1*, lysophospholipase 1; *MMP1A*, matrix metalloproteinase 1A; *NR1H3*, nuclear receptor subfamily 1 group H member 3; *PDGFRB*, platelet-derived growth factor receptor, β polypeptide; *TNC*, tenascin.

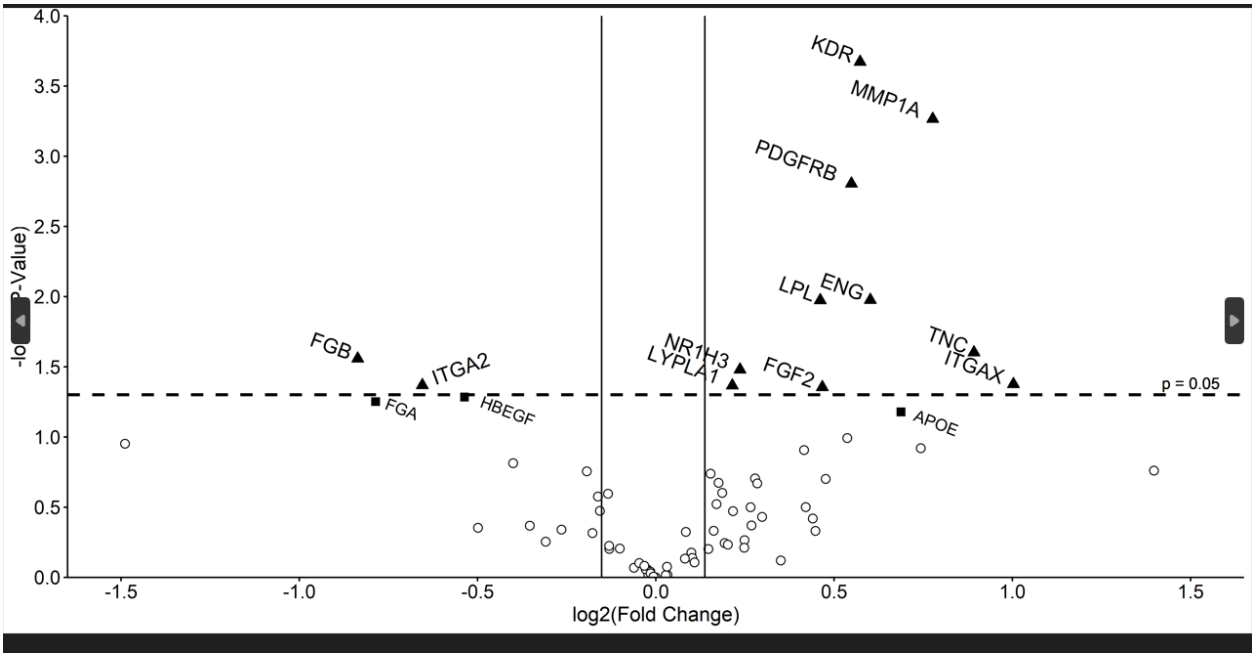

Figure 7. The effect of (+)-catechin hydrate on cell populations within the BM

Cell populations were assessed in the BM of mice after 21 days of HFD and treatment with either vehicle or 200 mg/kg/day (+)-catechin hydrate. The gating strategy is shown in Supplementary Fig. 5. Histograms show numbers (mean ± SEM) of WBC (A), MDSC (B), LSK (C), HPC1 (D), HPC2 (E), HSC (F), MPP (G), LK (H), CMP (I), GMP (J), MEP (K) and CLP (L). Statistical analysis was performed using Mann Whitney U test (group size of 8 for WBC, LSK, LK and CLP; 4 for MDSC, HPC1, HPC2, HSC, MPP, CMP, GMP and MEP); * $p \leq 0.05$, ** $p \leq 0.01$ or as stated. *Abbreviations*: CLP, common lymphoid progenitor; CMP, common myeloid progenitor; CLP, common lymphoid progenitor; GMP,

granulocyte-macrophage progenitor; HPC, hematopoietic progenitor cell; HSC, hematopoietic stem cells; LK, Lin^- c-Kit^+ cells; LSK, Lin^- $Sca1^+$ c-Kit^-; MDSC, myeloid derived suppressor cells; MEP, megakaryocyte-erythroid progenitor; MPP, multipotent progenitors; WBC, white blood cells.

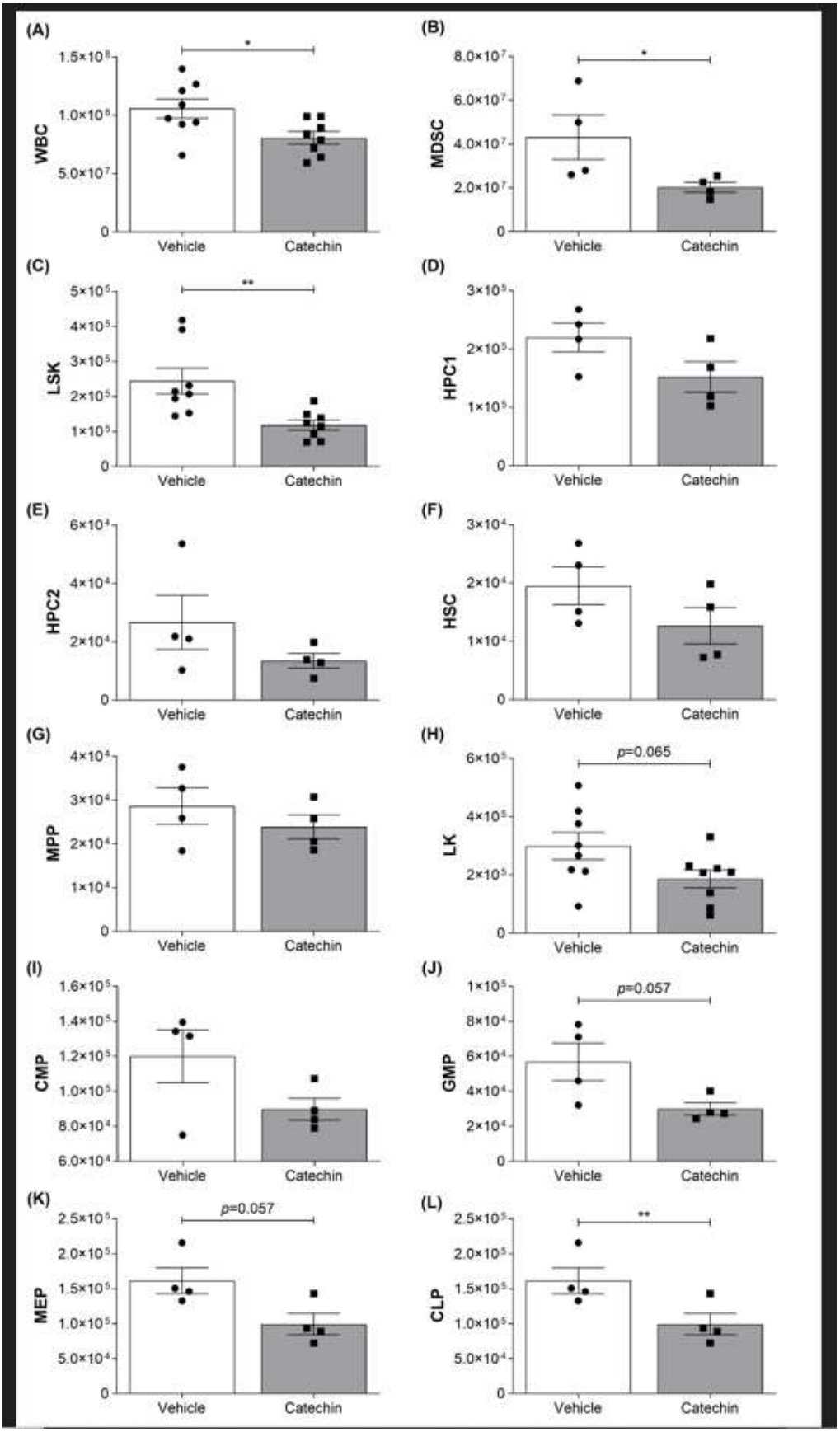

Figure 8. The effect of (+)-catechin hydrate on atherosclerotic plaque burden and lipid content

Male *LDLr*$^{-/-}$ mice were fed HFD supplemented with vehicle ('Control') or (+)-catechin hydrate ('Catechin') for 12 weeks. Sections of the aortic root at the three valve cusps were taken and stained with ORO. Images were captured using Leica DMRB microscope under x5 magnification and representative images with scale bars indicating 400 μm are shown in (A). Image analysis was performed using ImageJ software. Lipid content was calculated as percentage ORO^{+} staining within the plaque (B; n=22 for control and catechin); plaque content was calculated as percentage plaque area of vessel area (C; n=22 for control and n=21 for catechin) and occlusion (D; n=22 for control and n=21 for catechin) was calculated as percentage plaque area of lumen area. Total plaque area (E; n=23 for control and n=21 for catechin) and vessel area (F; n=22 for control and n=20 for catechin) are also shown. Statistical analysis was via an unpaired Student's t-test where *, $p \leq 0.05$ or as stated.

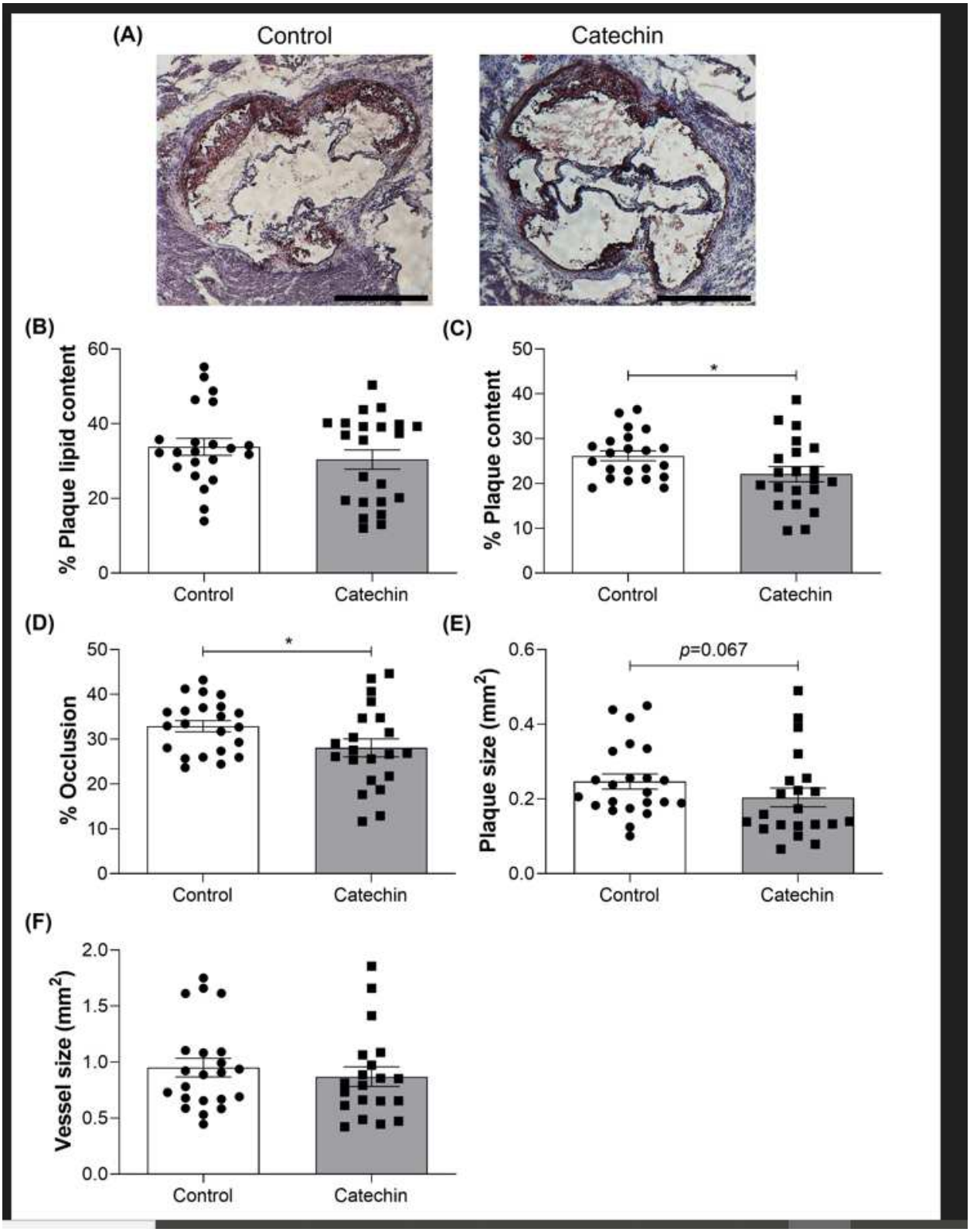

Figure 9. The effect of (+)-catechin hydrate on plaque immune cell infiltration

Male *LDLr*$^{-/-}$ mice were fed HFD supplemented with vehicle ('Control') or (+)-catechin hydrate ('Catechin') for 12 weeks. Immunofluorescence staining of the sections was used to

detect MOMA-2^{+} macrophages (B; n=16 for control and n=12 for catechin) and CD3^{+} T cells (C; n=18 for control and n=11 for catechin). Images were captured using Olympus BX61 microscope under x4 magnification and representative images with scale bars indicating 400 µm are shown in (A). Image analysis was performed using ImageJ software and statistical analysis was via an unpaired Student's t-test where ***, $p \leq 0.001$.

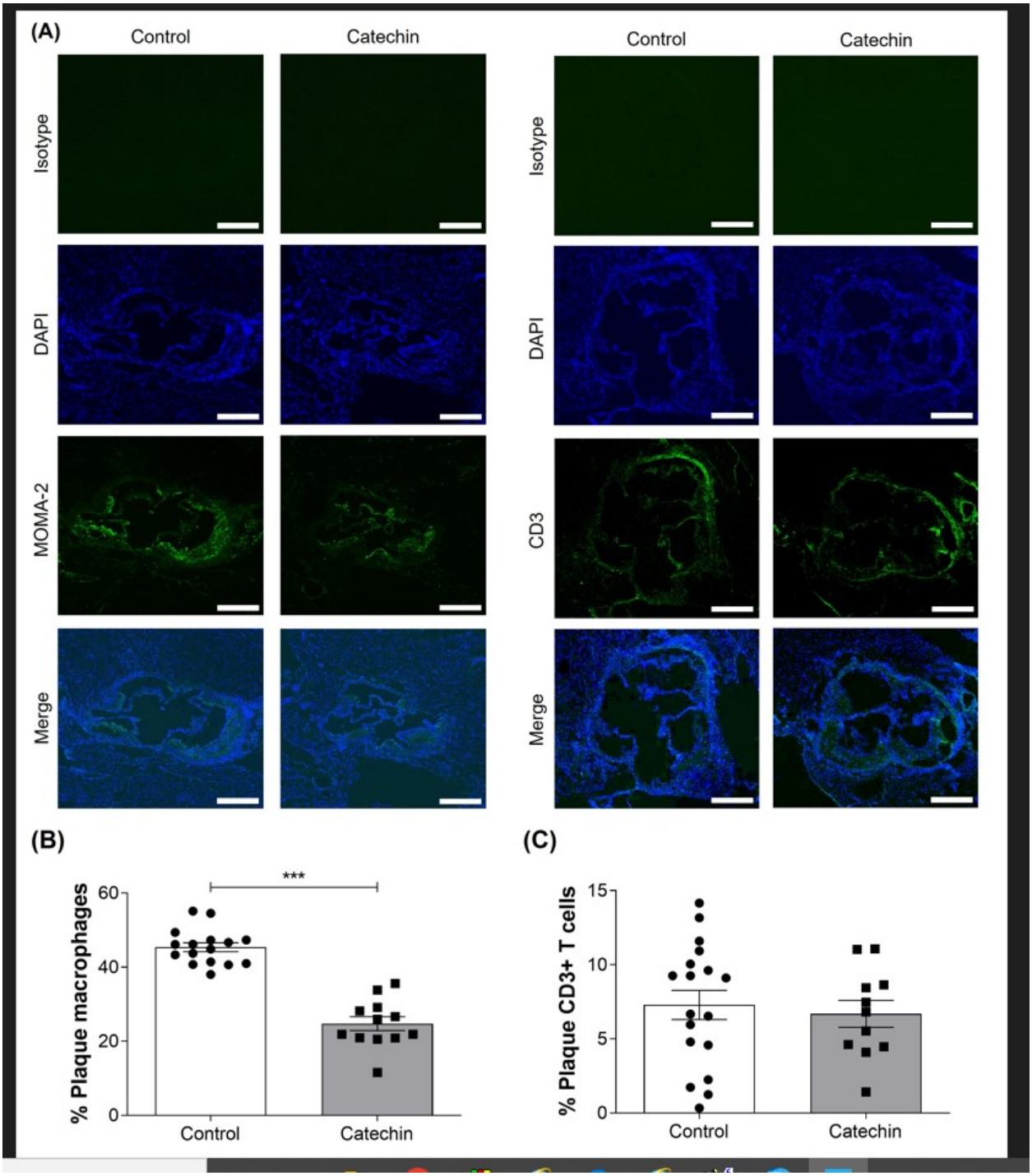

Figure 10. The effect of (+)-catechin hydrate on plaque necrosis and stability

Male *LDLr*$^{-/-}$ mice were fed HFD supplemented with vehicle ('Control') or (+)-catechin hydrate ('Catechin') for 12 weeks. Sections were stained with Van Geison's solution and captured using a Leica DMRB microscope at x5 magnification (A and C; n=21 for control and n=22 for catechin). Immunofluorescence staining of sections was used to detect α-smooth muscle actin (αSMA)$^{+}$ smooth muscle cells in plaque (B and D; n=16 for control and n=15 for catechin). Scale bars indicate 400 μm. Necrosis was calculated as acellular regions within plaque (E; n=23 for control and n=22 for catechin) and plaque stability index was calculated as (collagen + smooth muscle cells) / (lipid + macrophages) (F; n=20 for control and n=19 for catechin). Image analysis was performed using ImageJ software and statistical analysis was via an unpaired Student's t-test where *, $p \leq 0.05$.

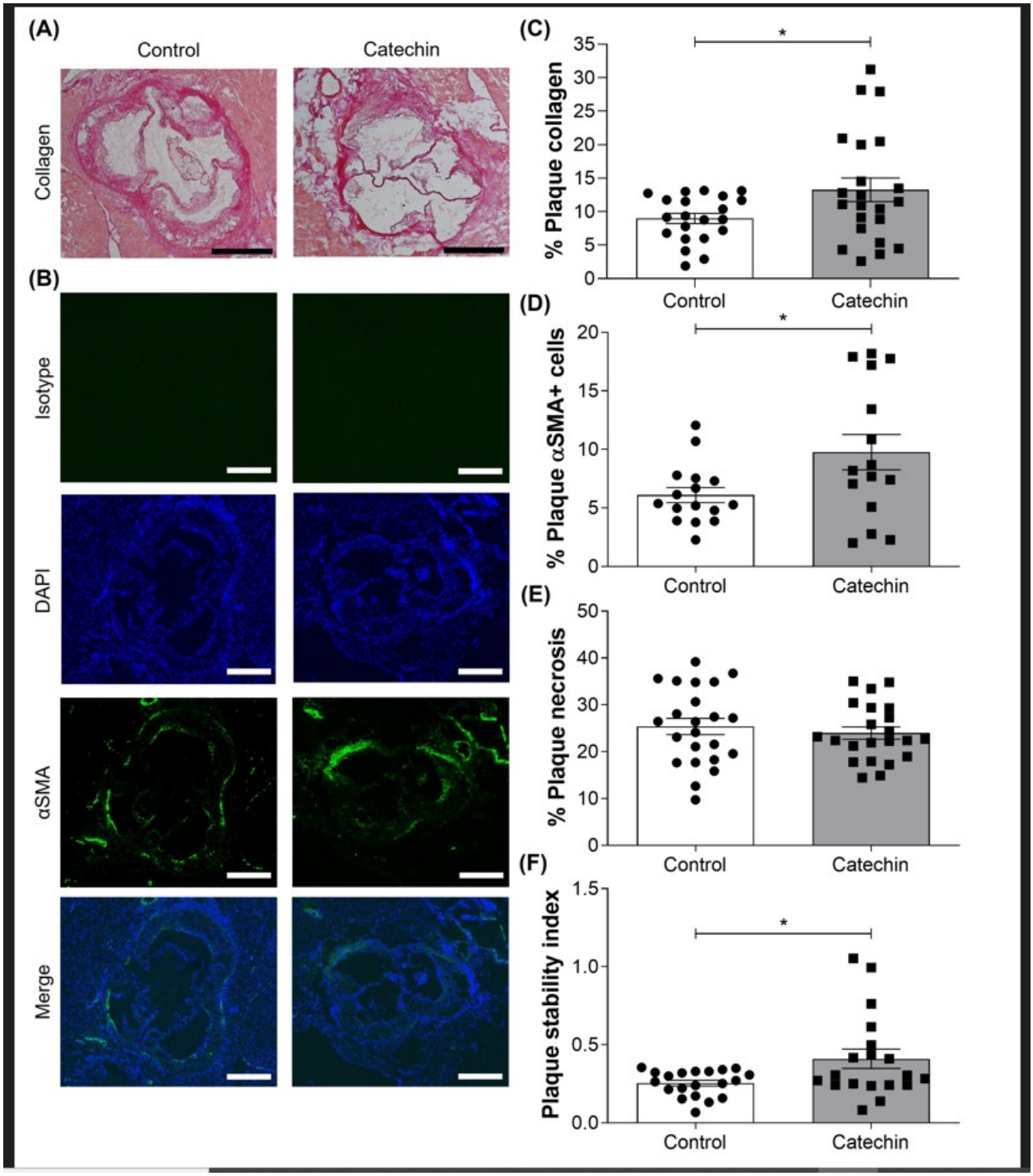

(+)-catechin attenuates atherosclerosis in LDL receptor deficient mice fed a high fat diet, several risk factors associated with the disease in C57BL6/J mice fed a high fat diet and prevents multiple processes associated with disease progression *in vitro*. Upward arrow, increase; downward arrow, decrease. CLP, common lymphoid progenitor; HFD, high fat diet; IL, interleukin; $LDLr^{-/-}$, Low density lipoprotein deficient mice; MDSC, myeloid-derived suppressor cells; oxLDL, oxidized LDL; ROS, reactive oxygen species; TG, triglyceride; WBC, white blood cells.

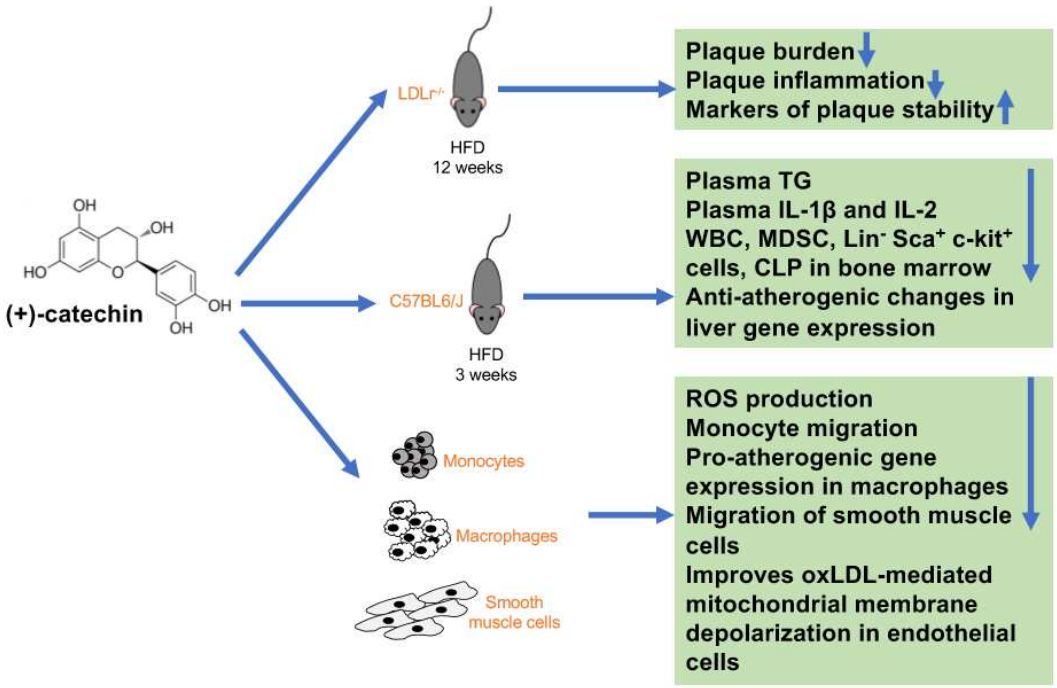

Table 1. The impact of (+)-catechin hydrate on plasma atherosclerosis-associated risk factors in C57BL/6J mice fed HFD

		Vehicle Control		Catechin	*p* value
	N	Mean ± SEM	N	Mean ± SEM	
Overall weight gain (g)	7	3.41 ± 0.25	8	5.19 ± 0.45	0.005
Adipose tissue deposits (mg)					
Total	8	39.95 ± 4.16	8	63.71 ± 4.56	0.002
Total white	8	36.38 ± 3.78	8	59.76 ± 4.36	0.001
Brown	8	3.56 ± 0.44	8	3.95 ± 0.47	0.561
Subcutaneous	7	12.72 ± 1.26	7	20.83 ± 1.16	$p \leq 0.001$
Gonadal	8	16.73 ± 2.04	8	27.51 ± 2.08	0.002
Inguinal	7	2.46 ± 0.16	7	2.62 ± 0.24	0.580
Renal	8	3.47 ± 0.77	8	7.86 ± 0.98	0.003
Lipids (mg/dl)					
TC	8	301.09 ± 19.47	8	348.72 ± 22.37	0.155
LDL/VLDL	8	92.70 ± 6.94	8	117.42 ± 14.40	0.170

HDL	8	30.84 ± 2.00	8	36.67 ± 2.90	0.158
Free cholesterol	7	43.62 ± 11.60	8	56.80 ± 14.73	0.526
TG	7	73.59 ± 1.53	8	66.06 ± 2.72	0.036
Lipid Ratios					
TC:HDL	8	9.48 ± 0.82	8	9.85 ± 0.80	0.765
TC:LDL/VLDL	8	3.37 ± 0.31	8	3.36 ± 0.43	0.992
LDL/VLDL:HDL	8	2.98 ± 0.32	8	3.23 ± 0.33	0.612
TG:TC	8	0.26 ± 0.02	8	0.20 ± 0.02	0.025
TG:HDL	8	2.42 ± 0.16	8	1.94 ± 0.22	0.120
TG:LDL/VLDL	8	0.87 ± 0.07	8	0.65 ± 0.10	0.119
Cytokines (pg/ml)					
IFN-γ	7	0.72 ± 0.22	8	0.91 ± 0.39	0.674
IL-10	8	19.76 ± 1.98	7	13.01 ± 1.83	0.025
IL-1β	7	1.17 ± 0.23	7	0.58 ± 0.09	0.032
IL-2	7	0.84 ± 0.04	5	0.53 ± 0.08	0.005
IL-4	3	0.36 ± 0.15	4	0.16 ± 0.03	0.182
IL-5	8	4.34 ± 0.61	8	3.23 ± 0.64	0.231
IL-6	8	199.1 ± 86.62	8	77.46 ± 31.41	0.208
CXCL1	8	396.5 ± 101.50	6	274.3 ± 65.28	0.344
TNF-α	8	17.12 ± 2.96	8	11.71 ± 21.68	0.163

The analysis was carried out on the plasma of C57BL/6J mice after 21 days feeding of HFD and daily gavage of vehicle or 200 mg/kg/day of (+)-catechin hydrate. Data for adipose tissue deposits have been normalized to body weight. Data (mean ± SEM) are from the indicated numbers of mice (any undetectable assay readings were removed prior to statistical analysis). Statistical analysis was performed using an unpaired Student's t-test (equal variance; log-transformed data used for IL-1β, IL-6 and CXCL1). *Abbreviations:* TC, total cholesterol; HDL, high-density lipoprotein; LDL/VLDL, low-density lipoprotein/very low-density lipoprotein, TG, triacylglycerol; IFN, interferon; IL, interleukin; TNF, tumour necrosis factor.

Table 2. The impact of (+)-catechin hydrate on plasma atherosclerosis-associated risk factors in *LDLr*$^{-/-}$ mice fed HFD

	Vehicle Control				Catechin				*p* value
	N	Mean	±	SEM	N	Mean	±	SEM	
Overall weight gain (g)	19	6.80	±	0.43	19	6.41	±	0.36	0.488
Adipose tissue deposits (mg)									
Total	19	52.43	±	4.95	18	45.39	±	3.86	0.273
Total white	19	48.94	±	4.86	18	41.74	±	3.80	0.255
Brown	19	3.49	±	0.24	20	3.54	±	0.26	0.903
Subcutaneous	19	16.31	±	1.49	18	13.68	±	1.01	0.157
Gonadal	19	23.41	±	2.47	18	20.78	±	2.13	0.427
Inguinal	19	1.27	±	0.18	19	1.21	±	0.17	0.772
Renal	20	8.32	±	1.10	19	6.37	±	0.80	0.162
Lipids (mg/dl)									
TC	19	1120.00	±	45.14	20	1264.00	±	53.92	0.013
LDL/VLDL	19	183.70	±	19.84	19	170.5	±	16.27	0.818
HDL	19	58.87	±	7.84	20	56.58	±	4.68	0.771
Free cholesterol	19	721.90	±	46.83	20	768.00	±	43.94	0.804
TG	18	61.73	±	5.91	18	48.84	±	3.88	0.077
Lipid Ratios									
TC:HDL	20	25.32	±	3.51	20	25.10	±	2.15	0.957
TC:LDL/VLDL	19	6.47	±	0.66	20	8.25	±	0.78	0.113
LDL/VLDL:HDL	20	3.72	±	0.39	19	3.12	±	0.23	0.196
TG:TC	19	0.05	±	0.01	19	0.04	±	0.00	0.043
TG:HDL	19	1.33	±	0.22	19	0.99	±	0.10	0.167
TG:LDL/VLDL	19	0.37	±	0.05	19	0.33	±	0.04	0.505
Cytokines (pg/ml)									
IFN-γ	18	0.30	±	0.02	19	0.39	±	0.04	0.048
IL-10	20	27.33	±	1.99	20	29.63	±	1.99	0.419
IL-1β	18	2.38	±	0.40	20	3.66	±	0.60	0.093
IL-2	20	1.28	±	0.06	19	1.44	±	0.17	0.728
IL-5	19	3.21	±	0.29	19	2.48	±	0.20	0.048
IL-6	19	89.43	±	17.48	18	158.5	±	31.55	0.066
CXCL1	19	203.3	±	39.10	19	253.8	±	44.01	0.418
TNF-α	18	15.09	±	1.33	19	15.06	±	0.99	0.964

The analysis was carried out on the plasma of *LDLr*$^{-/-}$ mice after 12 weeks feeding of HFD supplemented with either vehicle or 200 mg/kg/day (+)-catechin hydrate. Data for adipose tissue deposits have been normalized to body weight. Data (mean ± SEM) are from the indicated numbers of mice (any undetectable assay readings were removed prior to statistical analysis). Statistical analysis was performed using an unpaired Student's t-test (for adiposity parameters except inguinal adipose tissue, lipid levels except total and LDL/VLDL cholesterol, lipid ratios except TC:LDL/VLDL and TG:TC and cytokine levels except IL-2, CXCL1 and TNF-α) or Mann-Whitney U test (for all the others). *Abbreviations:* TC, total cholesterol; HDL, high-density lipoprotein; LDL/VLDL, low-density lipoprotein/very low-density lipoprotein, TG, triacylglycerol; IFN, interferon; IL, interleukin; TNF, tumour necrosis factor.